1 # Multiple horizontal mini-chromosome transfers drive
2 # genome evolution of clonal blast fungus lineages

3

4 A. Cristina Barragan[1]†*, Sergio M. Latorre[2]†, Angus Malmgren[1], Adeline Harant[1], Joe Win[1], Yu Sugihara[1],
5 Hernán A. Burbano[2], Sophien Kamoun[1]*, Thorsten Langner[1,a]*

6

7 [1]The Sainsbury Laboratory, University of East Anglia, Norwich Research Park, Norwich, UK
8 [2]Centre for Life's Origins and Evolution, Department of Genetics, Evolution and Environment,
9 University College London, UK
10 [a]Current address: Max Planck Institute for Biology, 72076, Tübingen, Germany

11

12 †Authors contributed equally, *Co-corresponding authors:
13 anacristinabl@gmail.com, sophien.kamoun@tsl.ac.uk, thorsten.langner@tuebingen.mpg.de

14

15 ## Abstract

16 Crop disease pandemics are often driven by clonal lineages of plant pathogens that reproduce asexually.
17 How these clonal pathogens continuously adapt to their hosts despite harboring limited genetic variation,
18 and in absence of sexual recombination remains elusive. Here, we reveal multiple instances of horizontal
19 chromosome transfer within pandemic clonal lineages of the blast fungus *Magnaporthe* (Syn. *Pyricularia)*
20 *oryzae*. We identified a horizontally transferred 1.2Mb supernumerary mini-chromosome which is
21 remarkably conserved between *M. oryzae* isolates from both the rice blast fungus lineage and the lineage
22 infecting Indian goosegrass (*Eleusine indica*), a wild grass that often grows in the proximity of cultivated
23 cereal crops. Furthermore, we show that this mini-chromosome was horizontally acquired by clonal rice
24 blast isolates through at least nine distinct transfer events over the past three centuries. These findings
25 establish horizontal mini-chromosome transfer as a mechanism facilitating genetic exchange among
26 different host-associated blast fungus lineages. We propose that blast fungus populations infecting wild
27 grasses act as genetic reservoirs that drive genome evolution of pandemic clonal lineages that afflict cereal
28 crops.

29

30

31 **Keywords:** Clonal blast fungus lineages, crop disease pandemics, horizontal mini-chromosome transfer,
32 wild hosts, genetic reservoirs

Introduction

Coevolutionary dynamics between plants and their pathogens date back millions of years and are a central force shaping both sets of genomes (Barragan and Weigel 2021). In such antagonistically interacting organisms, a cycle of adaptation and counter-adaptation must occur to avoid extinction (Van Valen 1973). This evolution relies not only on the acquisition of novel mutations but also on the preservation of long-standing genetic variation; together, these components provide the genetic foundations upon which selective pressures act (Nei 2007; Barrett and Schluter 2008). In eukaryotes, one of the major sources of genetic variation is recombination through sexual mating, yet many organisms, including fungal plant pathogens, preferentially reproduce asexually (Barrett 2010; Möller and Stukenbrock 2017). The absence of sexual recombination necessitates alternative mechanisms for generating genetic variability, including mutations, genomic rearrangements, transposon insertion, and gene duplication or loss (Seidl and Thomma 2014; Oggenfuss et al. 2023). However, these processes rely primarily on pre-existing genetic variation, and without the introduction of new genetic material, the adaptive potential of an asexual population is constrained. How clonal plant pathogens adapt to their hosts and avoid extinction despite harboring limited genetic variation is an important research question with practical implications, as clonal lineages of plant pathogens often drive disease pandemics in crops (Drenth et al. 2019).

One mechanism for acquiring genetic variation which does not require sexual mating, is horizontal gene transfer (HGT). This process, consisting of the transmission of genetic material from a donor to a recipient organism within the same generation, is considered a major force in preventing extinction in asexual organisms (Takeuchi et al. 2014). In prokaryotes, HGT is well-established as a source of genetic diversity, occurring through known mechanisms such as conjugation, transformation, or transduction (Sun 2018). The prevalence of HGT in eukaryotes has also become more apparent in recent years (Gabaldón 2020), particularly within the fungal kingdom – one of the most extensively studied eukaryotic lineage (Fitzpatrick 2012; Mohanta and Bae 2015; Sahu et al. 2023). In fungi, parasexuality, a mechanism enabling chromosome reassortment independent of sexual reproduction (Nieuwenhuis and James 2016), is a plausible avenue for HGT.

Fungal genes acquired by HGT are often part of the non-essential accessory genome which is variable between individuals of the same species and contrasts to the core genome, which contains genes essential to housekeeping functions (McCarthy and Fitzpatrick 2019). This is in line with the "two-speed" genome model observed in some filamentous plant pathogens (fungi and oomycetes), where indispensable genomic regions are under higher evolutionary constraints and may appear as slow-evolving, while variable genomic regions are under more relaxed constraints or positive selection, and can appear as rapidly-evolving (Dong et al. 2015). Rapidly-evolving or dynamic genome compartments are characterized by the presence of virulence genes, high sequence diversification, presence/absence variation, structural changes, and segmental duplications (Torres et al. 2020; Huang et al. 2023). An extreme form of structural variation are mini-chromosomes (mChr), also referred to as supernumerary, accessory, or B chromosomes, which exist in addition to core chromosomes and have been found in 15% of eukaryotic species (Covert 1998). While mChr emergence has been associated with genomic rearrangements at repeat- and effector-rich subtelomeric ends of core chromosomes (Bertazzoni et al. 2018; Peng et al. 2019; Langner et al. 2021; van Westerhoven et al. 2023), the exact molecular mechanism remain an area of ongoing investigation. By being physically unlinked from core chromosomes, mChr can diversify rapidly and could serve as a cradle for adaptive evolution without compromising genomic integrity (Croll and McDonald 2012).

2

77   The adaptive role of mChr in plant pathogenic fungi is underpinned by their correlation to virulence in
78   various pathogen-host systems (Miao et al. 1991; Kistler 1996; Han et al. 2001; Akagi et al. 2009; Ma et al.
79   2010; Chuma et al. 2011; Balesdent et al. 2013; van Dam et al. 2017; Habig et al. 2017; Bhadauria et al.
80   2019; Henry et al. 2021; Asuke et al. 2023). In addition, variation in virulence has been partly attributed
81   to the horizontal transfer of mChr (Mehrabi et al. 2011). This is exemplified in the case of *Fusarium*
82   *oxysporum*, where the horizontal acquisition of a mChr in laboratory settings transformed a non-
83   pathogenic strain into a virulent pathogen (Ma et al. 2010). Similarly, in the insect pathogen *Metarhizium*
84   *robertsii,* strains with a horizontally acquired mChr were more virulent compared to those without this
85   mChr (Habig et al. 2023).
86
87   A notorious plant pathogenic fungus where asexually reproducing clonal lineages underlie crop pandemics,
88   is the blast fungus *Magnaporthe oryzae* (Syn. *Pyricularia oryzae*) (Latorre et al. 2020; Latorre et al. 2023).
89   The blast fungus is one of the most devastating plant pathogens worldwide and is the causal agent of blast
90   disease in dozens of wild and cultivated grasses (Islam et al. 2023). As a species*, M. oryzae* is differentiated
91   into genetic lineages that tend to be host-associated, with occasional gene flow observed between certain
92   lineages (Couch et al. 2005; Gladieux, Condon, et al. 2018). The highly destructive rice blast fungus lineage
93   reproduces mostly asexually in nature, with limited traces of sexual reproduction having been found (Saleh
94   et al. 2012; Thierry et al. 2022). Nevertheless, the rice blast fungus lineage remains genetically isolated,
95   with no gene flow detected from other *M. oryzae* lineages so far (Gladieux, Condon, et al. 2018). To date,
96   three globally prevalent clonal lineages affecting rice and one affecting wheat have been identified as the
97   underlying cause of persistent blast pandemics (Latorre et al. 2020; Latorre et al. 2023). Despite their
98   restricted genetic diversity, clonal *M. oryzae* lineages readily evolve to counteract host defenses, posing a
99   challenge to the development of durable blast-resistant crop varieties (Younas et al. 2023). The mechanism
100   that allows clonal blast fungus populations to adapt to new host germplasm, despite an apparent lack of
101   avenues for genetic innovation, remains elusive.
102
103   Structural variation in both mChr and core chromosomes contribute to genomic diversity in the blast
104   fungus (Talbot et al. 1993; Orbach et al. 1996). Recent genomic analysis of a wheat blast fungus isolate
105   revealed multi-megabase insertions from a related species, suggesting HGT (Kobayashi et al. 2023). In
106   addition, the postulated horizontal transfer of the avirulence gene AVR-Pita2 among related species to the
107   blast fungus substantiates the hypothesis that HGT is occurring (Chuma et al. 2011). While these instances
108   highlight HGT as a possible driver of genetic variation in the blast fungus, the exact mechanisms facilitating
109   HGT remain unclear. In addition to gene transfer, mChr have been associated with virulence gene
110   reshuffling and recombination with core chromosomes (Kusaba et al. 2014; Peng et al. 2019; Langner et
111   al. 2021; Asuke et al. 2023; Gyawali et al. 2023), indicating that horizontal mChr transfer could be
112   instrumental in driving genomic innovation.
113
114   In this study, we provide evidence for multiple horizontal mini-chromosome transfer events involving
115   clonal lineages of the rice blast fungus *M. oryzae* that occurred under field conditions. We identified a
116   1.2Mb supernumerary mini-chromosome, mChrA, which is remarkably conserved across *M. oryzae*
117   isolates from lineages infecting the wild host species, Indian goosegrass (*Eleusine indica*), and rice. We show
118   that mChrA was acquired by clonal rice blast fungus lineages through at least nine independent horizontal
119   transfer events over the past three centuries. This establishes horizontal mChr transfer as a naturally
120   occurring genetic exchange mechanism among different host-associated blast fungus lineages. Our findings

121 lead us to propose that blast fungus lineages infecting wild grasses serve as genetic reservoirs, driving
122 genome evolution of pandemic asexual clonal lineages that afflict crops.
123
Results
Clonal rice blast fungus isolates display variable mChr content
126 We have previously shown that genetically diverse *M. oryzae* isolates exhibit variable mChr content
127 (Langner et al., 2021). Here, we set out to analyze the extent to which mChr variation contributes to
128 genomic diversity in a set of genetically related isolates belonging to a single clonal lineage. To this end,
129 we selected nine rice blast fungus isolates collected from Italy (Win et al. 2020) (**Fig S1A** and **Table**
130 **S1**). Using genome-wide single-nucleotide polymorphism (SNP) data we confirmed that the nine isolates
131 belong to a single clonal lineage (clonal lineage II), which is predominant in Europe (Latorre et al. 2020;
132 Thierry et al. 2022) (**Fig 1A**, **S1B** and **Table S2**).
133
134 To determine the karyotype of the selected isolates, we performed contour-clamped homogeneous
135 electric field based (CHEF) electrophoresis. This revealed variable numbers and sizes of mChr, with each
136 isolate exhibiting one to four mChr, each varying from 0.5 to 2Mb in size (**Fig 1B** and **1C**). To genetically
137 characterize individual mChr, we performed mini-chromosome isolation sequencing (MCIS) on all
138 eighteen mChr found across the nine isolates (Langner et al. 2019; Langner et al. 2021). Reads obtained
139 from each individual mChr were mapped to the reference assembly corresponding to its originating
140 isolate. Contigs exhibiting high MCIS coverage and high repeat density, a characteristic trait of mChr, and
141 were <2Mb in size, were identified as mChr contigs (**Fig S2**, **S3**, **Table S3** and **S4**).
142
143 Next, we compared mChr contigs across the studied clonal isolates. Reciprocal sequence homology
144 searches revealed the presence of a conserved 1.7Mb mChr (mChrC) in eight out of the nine isolates.
145 mChrC corresponds to a previously identified mChr found in the rice blast fungus isolate FR13, which
146 also belongs to clonal lineage II (Langner et al. 2021). We aligned mChrC contigs and confirmed high
147 synteny across isolates (**Fig 1D**). To obtain an overview of how common mChrC is in the global *M.*
148 *oryzae* population, we examined the presence of this sequence across 413 *M. oryzae* and *Magnaporthe*
149 *grisea* isolates (**Table S5**). We performed short-read mapping to the AG006 genome, known from
150 karyotyping to possess the highest mChr diversity. Subsequent breadth of coverage calculations (see
151 Methods) revealed that mChrC is particularly conserved among rice blast fungus isolates, especially those
152 belonging to clonal lineage II (**Fig S4A-C** and **Table S6**).
153
154 *M. oryzae* isolate AG006 stood out within the examined set of isolates as it contained three additional
155 mChr named mChrS, mChrA, and mChrM, in addition to mChrC. These mChr exhibited sizes ranging
156 from 0.97 to 2Mb. Notably, the largest of these mChr, which we termed the mosaic mini-chromosome
157 (mChrM), was composed of segments derived from the three smaller mChr, namely, mChrC, mChrA,
158 and mChrS (**Fig 1B**, **1C**, **1E** and **S2**). The presence of this mosaic mChr reveals that recombination
159 among mChr occurs, and plays a role in generating novel genetic combinations.
160
161 Upon closer examination of mChrA, we found it exhibited low sequence similarity to the genomes of the
162 other Italian isolates, as evidenced by reciprocal sequence homology searches (**Fig 1B**, **1C**, **1E** and
163 **Table S7** and **S8**). There were two exceptions to this, a duplicated fragment within mChrM (**Fig 1E**),
164 and a small 0.1Mb contig (AG006_Contig17) which aligned to a specific region of mChrA

165   (AG006_Contig10) (**Fig S3A**). The latter may have originated from a sequence duplication event or be
166   an assembly artifact. mChrA displayed high MCIS coverage and canonical telomeric repeats at both ends,
167   indicating it is linear and largely assembled into a single contig (**Fig S5**). Lastly, to reinforce these findings,
168   we conducted a whole-genome alignment between AG006 and AG002, an isolate genetically highly similar
169   to AG006 (**Fig S1B**), confirming the absence of mChrA in AG002 (**Fig 2F**).

171   Taken together, we found high mChr diversity in a collection of nine clonal rice blast fungus isolates.
172   Remarkably, we identified a unique mChr, mChrA, which does not display sequence similarity to the other
173   nine rice blast fungus isolates. This finding underscores the unique genetic variation present even among
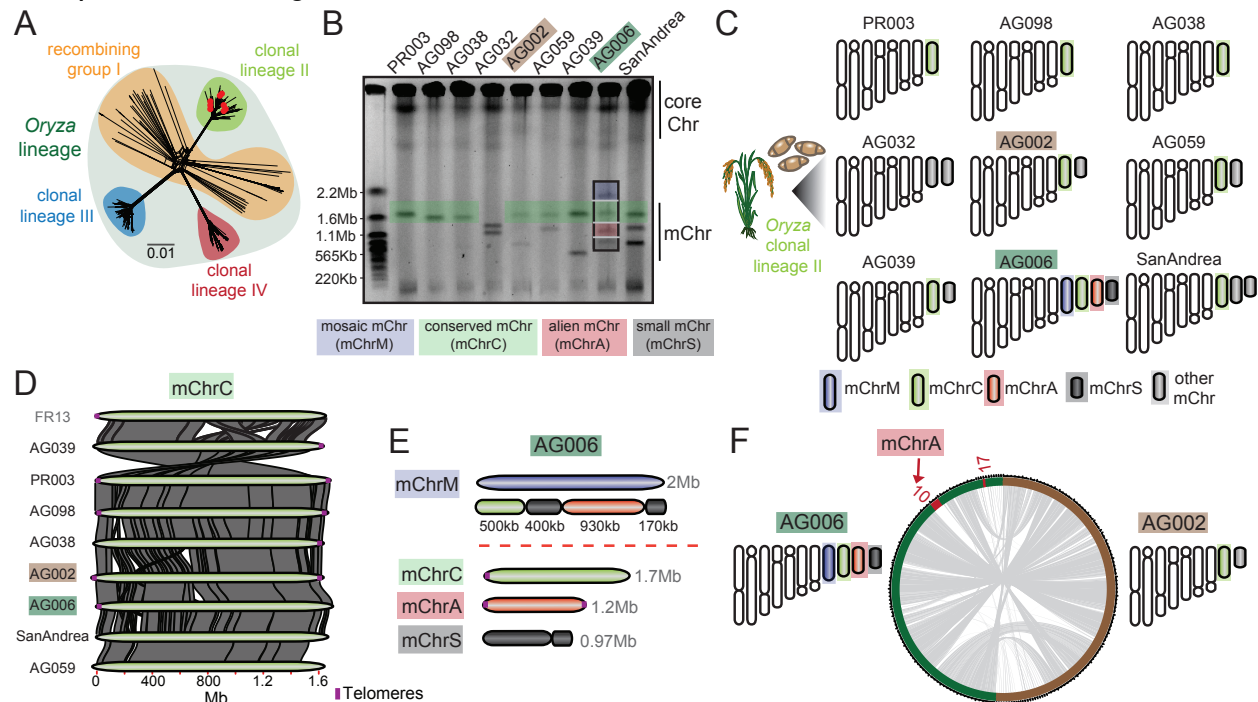174   closely related blast fungus isolates.

175
176   **Fig 1. Clonal rice blast fungus isolates display variable mChr content. A.** Genome-wide SNP-based
177   NeighborNet analysis confirms the nine rice blast fungus isolates (red dots) belong to clonal lineage II (green) (Latorre
178   et al. 2020). **B.** CHEF gel karyotyping reveals variable mChr content. A conserved 1.7Mb mChr (mChrC, green) is
179   found in eight of nine isolates. A 2Mb mChr (mChrM, blue), present in isolate AG006, is a mosaic composed of
180   fragments from three other mChr (mChrC, mChrA, and mChrS; see panel E) from the same isolate. A third 1.2Mb
181   mChr (mChrA, red) found in AG006, is absent from the genomes of the other isolates (see panels E and F). **C**.
182   Schematic karyotype of Italian isolates. Core chromosomes are shown in white. mChr studied in detail are highlighted
183   in colors, while the rest are in gray. **D.** mChrC exhibits high synteny across isolates and is also found in isolate FR13
184   (Langner et al. 2021). Telomeric sequences are indicated by a vertical line (purple). **E.** Inferred mChrM sequence
185   composition. **F.** Whole-genome alignment between AG006 (green) and AG002 (brown). mChrA (AG006_Contig10)
186   and AG006_Contig17 (in red) are absent from AG002.

188   **mChrA sequences are present across multiple host-associated blast fungus lineages**
189   To determine the origin of mChrA, we assessed the presence of the mChrA sequence (AG006_Contig10)
190   across a set of 413 *M. oryzae* isolates belonging to ten different host-associated lineages and to *M. grisea*
191   (**Fig 2A** and **Table S5**). For this purpose, we calculated the breadth of coverage for mChrA
192   (AG006_Contig10) in each isolate, and observed it followed a bimodal distribution (**Fig 2B**). Model-based
193   clustering established 126 isolates as mChrA carriers (**Fig S6A-B** and **Table S9**, see Methods). These
194   isolates belonged to six different host-associated *M. oryzae* lineages (**Fig 2A, B** and **S6D**). Notably, only

195   12% of rice blast fungus isolates (32 of 276) were identified as mChrA carriers (**Fig 2A**, **B** and **Table**
196   **S9**). These rice blast fungus isolates were genetically diverse, belonging to all three clonal lineages and the
197   recombining group (defined here as *Oryza* subgroups) (**Fig 2C** and **S6E**).
198
199   In contrast to rice blast fungus isolates, the mChrA sequence was common across isolates belonging to
200   the *Lolium* and *Triticum* lineages, with most isolates carrying 80-90% of the mChrA sequence (**Fig 2B** and
201   **S6D**). Previous karyotyping and sequencing efforts identified isolate B71 from the *Triticum* lineage and
202   isolate LpKY97 from the *Lolium* lineage to carry mChr (Peng et al. 2019; Rahnama et al. 2020). Given that
203   these isolates also carry a substantial portion of the mChrA sequence (79% and 87% mapping to mChrA
204   in AG006, respectively), it suggests that the mapped mChrA sequences may share a common ancestry
205   with the mChr in these two isolates. However, the most striking sequence identity was observed in two
206   isolates from the *Eleusine* blast fungus lineage, Br62 and B51. These exhibited mChrA coverage comparable
207   to the rice blast fungus isolate AG006, suggesting high similarity in the mChrA sequences between these
208   isolates (**Fig 2B** and **Table S6**). Taken together, mChrA sequences were found in blast fungus isolates
209   belonging to six different host-associated lineages, with members of the *Eleusine* and *Oryza* lineages
210   carrying nearly identical mChrA sequences.
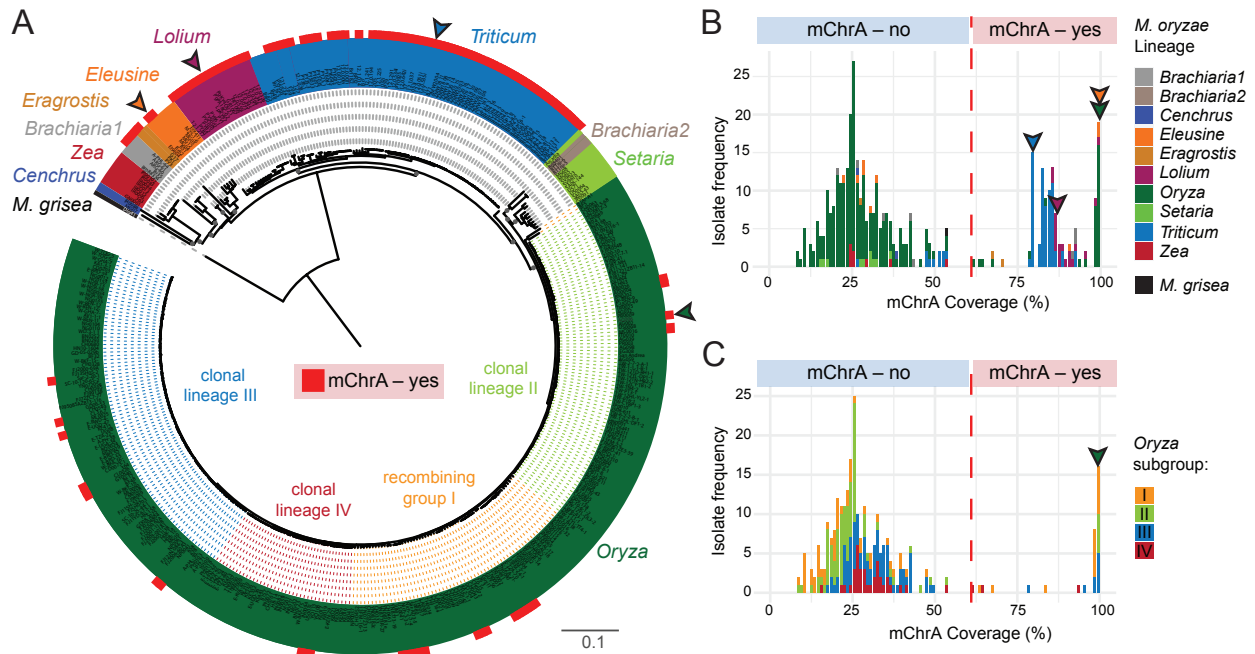
211
212   **Fig 2. mChrA sequences are present across multiple host-associated blast fungus lineages. A.**
213   Genome-wide SNP-based NJ tree of 413 *M. oryzae* and *M. grisea* isolates. *M. oryzae* isolates are color-coded by
214   lineage and *M. grisea* is in black. The 126 isolates defined as mChrA carriers (Table S9) are highlighted by a red square
215   and belong to six different *M. oryzae* lineages. Arrows indicate isolates with mChrA-related karyotyping information
216   (Peng et al. 2019; Rahnama et al. 2020), see Fig 4). Colors of dotted lines across the rice blast lineage represent
217   different genetic subgroups (three clonal lineages and a recombining group) (Latorre et al. 2020). Scale bar represents
218   nucleotide substitutions per position. **B.** Bimodal distribution of mChrA breadth of coverage across 413 *M.oryzae*
219   and *M. grisea* isolates. The coverage cutoff (61%) for mChrA presence or absence is indicated by the dotted red line.
220   Arrows as in A. **C.** mChrA breath of coverage across 276 rice blast fungus isolates. Colors represent different
221   genetic subgroups in the *Oryza* lineage. Arrows and coverage cutoff as in B.
222
223   **Discordant genetic clustering between the core genome and mChrA**

224   Given the patchy distribution of mChrA sequences across isolates from different host-associated blast
225   fungus lineages, we investigated the evolutionary relationships of their core genome and mChrA
226   sequences. Using SNP-based phylogenies and principal component analyses (PCA), we found a clear
227   discordance between the core genome and mChrA (**Fig 3A-D**). For the core genome, isolates are
228   clustered by lineage, whereas for mChrA, lineage-dependent clustering becomes less evident. Most
229   strikingly, whereas the core genomes of isolates from the *Oryza* and *Eleusine* lineages form two distinct
230   groups (**Fig 3A**, **B** and **S7A**), these two fall within a single group for mChrA (**Fig 3C**, **D** and **S7B**). This
231   shows that the mChrA sequence in isolates from these two lineages is highly similar, but their core genome
232   is divergent. We note that for the mChrA clustering, three clonal rice blast fungus isolates did not group
233   with other isolates from this lineage, possibly reflecting mChrA sequence dissimilarity.
234
235   To ascertain the robustness of the observed genetic clustering of mChrA between members of the *Oryza*
236   and *Eleusine M. oryzae* lineages, we generated phylogenies using 100 randomly selected genomic regions
237   of the same size as mChrA (1.2Mb) across the core genome of all 126 isolates. In all instances, the *Oryza*
238   lineage was monophyletic, and in zero instances did the *Oryza* and *Eleusine* lineages cluster together (**Fig
239   3E**). This demonstrates that the clustering of members of the *Eleusine* and rice blast fungus lineages is
240   highly unusual and limited to the mChrA sequence. To complement this analysis, we evaluated genetic
241   differentiation between isolates belonging to the rice and *Eleusine* blast fungus lineages carrying the mChrA
242   sequence by calculating the fixation index (F_{ST}) from genome-wide SNP data (Wright 1951). This analysis
243   confirmed high levels of inter-lineage genetic differentiation in the core genome, but low differentiation
244   levels for mChrA (**Fig 3E** and **S8**). We conclude that mChrA shows discordant genetic clustering when
245   compared to the core genome, which indicates contrasting evolutionary trajectories.
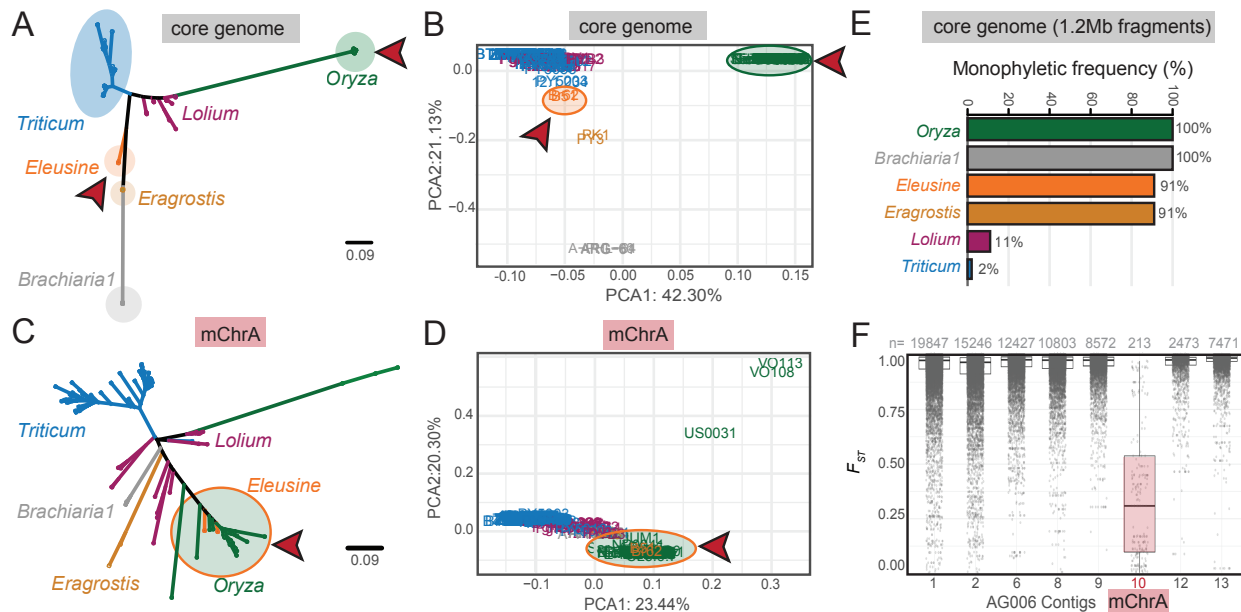
Fig 3. Discordant genetic clustering between the core genome and mChrA. A-D. SNP-based NJ trees (A and C) and Principal Component Analyses (PCA, B and D) of 126 *M. oryzae* isolates carrying the mChrA sequence. Discordance between core genome (A and B) and mChrA (C and D) genetic clustering is observed (red arrows). Scale bar represents nucleotide substitutions per position. **E.** Percentage of tree topologies where a monophyletic relationship was observed for 100 randomly selected 1.2Mb core-chromosomal regions. **F.** F_{ST} between rice blast fungus isolates (n=32) and isolates from the *Eleusine* lineage (Br62 and B51) both carrying mChrA. Each dot (gray) indicates the weighted F_{ST} per 5kb window using a step size of 500bp. The number of windows per contig are at the top of each box. Core chromosome contigs >2Mb and mChrA are shown.

Eleusine isolate Br62 and *Oryza* isolate AG006 carry an intact and highly syntenic mChrA

Following the identification of highly similar mChrA sequences in two isolates from the *Eleusine* blast fungus lineage, we aimed to determine whether these sequences originate from an intact mChr, or whether they are embedded within the core genome, as observed for mChrC segments in *M. oryzae* isolate 70-15 (Langner et al. 2021). To test this, we performed CHEF-gel based karyotyping, and found that Br62 possesses a single mChr of the same size (1.2Mb) as mChrA in AG006 (**Fig 4A**). We performed whole-genome sequencing of Br62 using both Illumina short reads and Nanopore long reads, followed by *de novo* whole-genome assembly (**Table S10**). Subsequent whole-genome alignment between AG006 and Br62 revealed that Br62_Contig07 corresponds to mChrA (AG006_Contig10) and AG006_Contig17 (**Fig 4B**). Furthermore, the alignment of the mChrA in both isolates revealed a high level of synteny, with a single re-arrangement in the center of mChrA (**Fig 4C**).

To independently validate these findings, we took advantage of a Br62 isolate that lost mChrA after subculturing, as determined by CHEF gel electrophoresis (**Fig S9A**). To identify contigs that originate from the mChr, we sequenced the genome of the Br62 isolate that lacks the 1.2Mb mChr (referred to as Br62-) using Illumina short-reads and aligned the reads to the Br62 genome. We calculated mapping depth per contig in Br62 and Br62-. Depths were consistent in both isolates except for Contig07, here Br62- displayed a near-zero read depth, indicating this corresponded to mChrA (**Fig S9B**). Additionally, Contig07 exhibited a high repeat content, a characteristic feature of mChr (**Fig S9C**). Together these analyses confirm the presence of an intact mChrA in Br62. Intriguingly, subculturing not only resulted in the loss of mChrA in Br62 but also in the loss of the mosaic mChrM in AG006 (**Fig 4A**), underlining the dynamic nature of mChr (Peng et al. 2019; Langner et al. 2021; Liu et al. 2022).

We next set out to determine whether the mChrA sequence is also found as an intact mChr in isolates belonging to other blast fungus lineages known to carry mChr (Peng et al. 2019; Rahnama et al. 2020), and which we identified as mChrA carriers (**Table S9**). We performed pairwise whole-genome alignments between AG006, isolate LpKY97 from the *Lolium* lineage, and isolate B71 from the *Triticum* lineage. Here, mChrA partially aligned to the mChr of both B71 and LpKY97, and to the end of chromosome 3 in B71, which was previously identified as a potential segmental duplication between the B71 mChr and core chromosomes (Peng et al. 2019; Liu et al. 2022; Gyawali et al. 2023) (**Fig 4C** and **Fig S10A-C**). The partial mChrA alignments are in accordance with our genetic clustering and breadth of coverage analyses, indicating that mChrA-like mChr are present in LpKY97 and B71, but these are structurally divergent from mChrA in AG006 and Br62 (**Table S6**). As a negative control, we aligned mChrA from AG006 to the conserved mChrC in the rice blast fungus isolate PR003 using the same parameters and no alignments were retrieved. We conclude that mChrA is present as an intact and highly syntenic mChr in the rice blast fungus isolate AG006 and in *Eleusine* blast fungus isolate Br62.
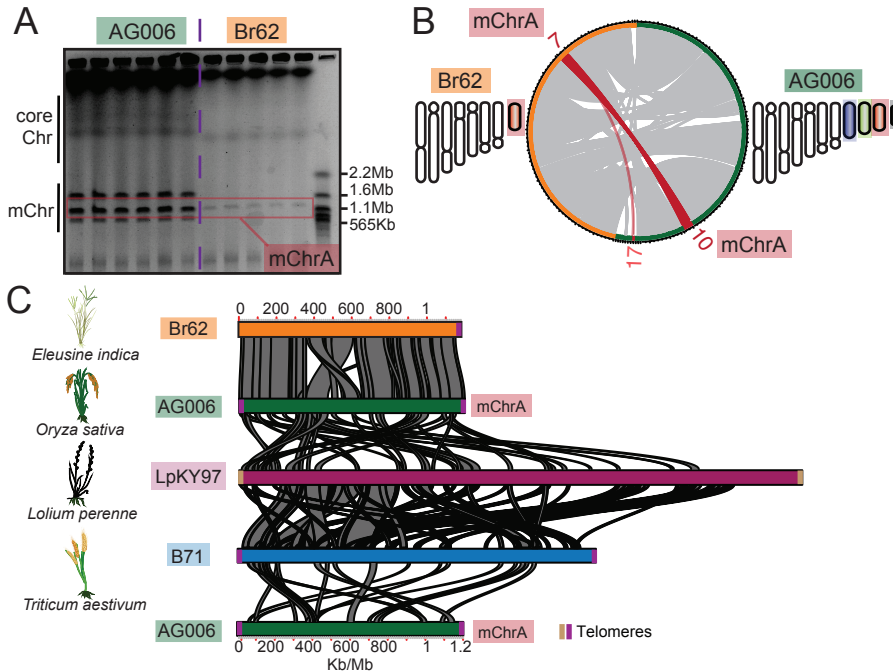
Fig 4. *Eleusine* isolate Br62 and *Oryza* isolate AG006 carry an intact and highly syntenic mChrA. A. CHEF-gel karyotyping of AG006 and Br62. Six gel lanes per isolate are shown representing a single biological replicate. Br62 carries a 1.2Mb mChr, the same size as mChrA in AG006 (in red). **B.** Whole-genome alignment of Br62 (orange) and AG006 (green). Br62_Contig07 aligns exclusively to mChrA (AG006_Contig10) and AG006_Contig17 (red). For both isolates a schematic karyotype is depicted. **C.** Alignment of mChrA in AG006 and Br62 reveal high synteny, except for a rearrangement in the central region. Alignments covering a fraction of mChrA are seen among mChrA in AG006 and the mChrA-like mChr1 in *Lolium* isolate LpKY97 (magenta) and the mChr in *Triticum* isolate B71 (blue). Telomeric sequences are indicated by vertical lines (purple/brown). The host plant of each isolate is shown on the left.

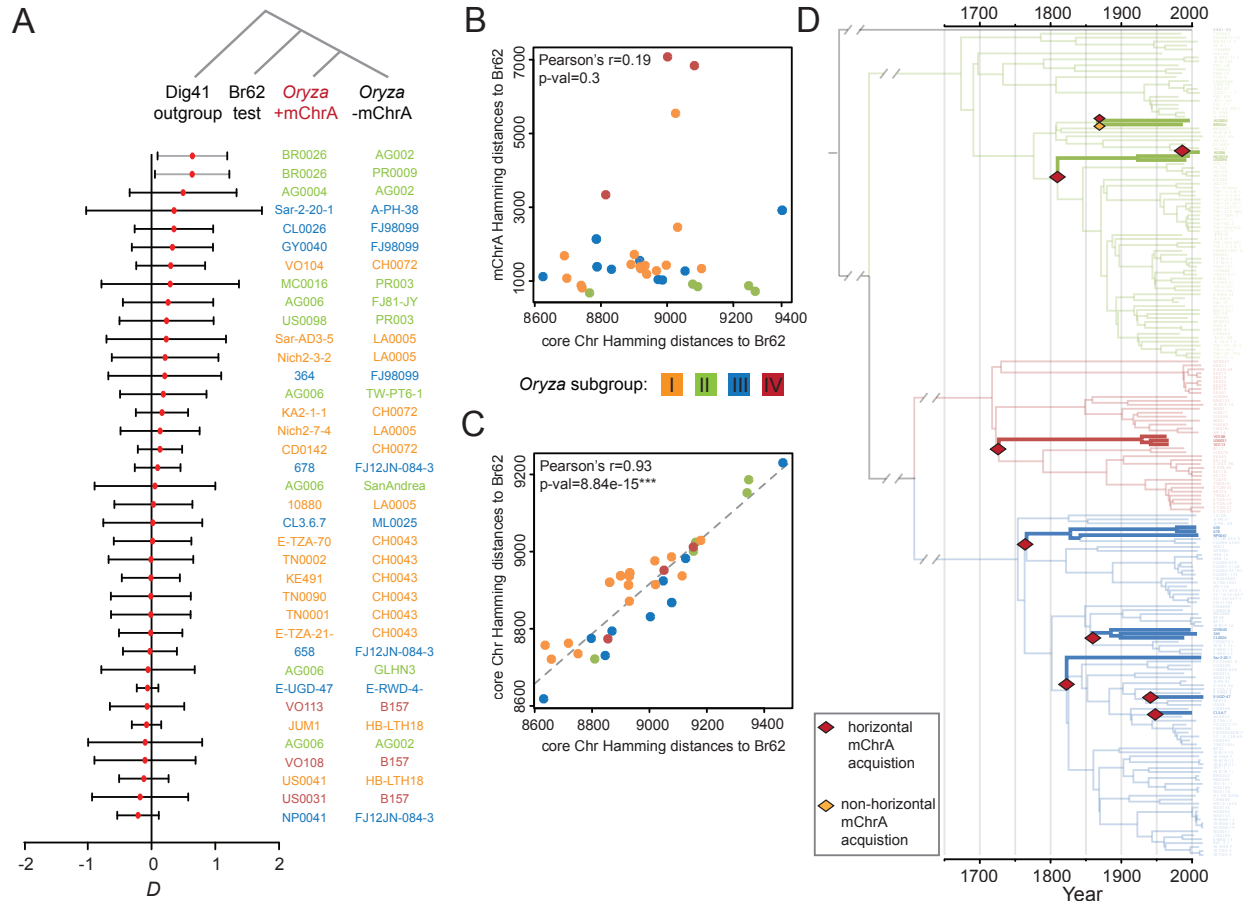**Multiple horizontal mChrA transfers occurred in clonal rice blast fungus lineages**

To test if sexual mating or horizontal gene transfer (HGT) can explain the presence of mChrA in the *Eleusine* and *Oryza* blast fungus lineages, we evaluated patterns of allele sharing through *D*-statistics (Green et al. 2010; Durand et al. 2011). After the mChrA sequence is removed from the genomes, we hypothesize that sexual mating results in a genome-wide introgression signal, leading to a *D*-statistic significantly different from zero, whereas HGT will not produce such a signal. Consequently, we first removed mChrA sequences, and then compared Br62 with the 32 rice blast fungus isolates carrying mChrA sequences, and 13 rice blast isolates not carrying this sequence (see Methods). For each comparison, rice blast fungus isolates belonging to the same *Oryza* subgroup were chosen. We selected *M. grisea* isolate Dig41 as an outgroup, which is divergent from both the rice and *Eleusine* blast fungus lineages. This resulted in the phylogenetic configuration: (Dig41, Br62; *Oryza* +mChrA, *Oryza* -mChrA). Under this configuration, a 99% confidence interval encompassing *D*=0 indicates there is no genome-wide introgression signal and favors the hypothesis of horizontal mChrA transfer. On the other hand, a 99% confidence interval not encompassing *D*=0 signals genome-wide introgression, supporting the acquisition of mChrA through sexual mating. In all tested configurations except those involving isolate BR0026 (31 of 32 isolates), the 99% confidence interval encompassed *D*=0, supporting the acquisition of mChrA by horizontal transfer (**Fig 5A** and **Table S11**). As a control, we tested the configurations (Dig41, Br62; *Oryza* +mChrA, *Oryza* +mChrA) (**Fig S11A**) and (Dig41, Br62; *Oryza* -mChrA, *Oryza* -mChrA) (**Fig S11B** and **Table S11**). Here, the 99% confidence interval encompassed *D*=0 in all tested configurations.

322   Having established that mChrA was likely horizontally acquired in the large majority of rice blast fungus
323   isolates carrying this sequence (31 of 32 isolates), and given its patchy distribution across the rice blast
324   fungus lineage, we sought to differentiate between a single ancestral mChrA acquisition followed by
325   independent losses, and multiple independent mChrA acquisitions. To test this, we estimated the genetic
326   distance between the mChrA sequence present in the 32 *Oryza* isolates and Br62 and compared it to the
327   genetic distance between random core chromosomal fragments of the same size as mChrA in the same
328   32 *Oryza* isolates (1.2Mb) and Br62. A significant correlation between the two genetic distances indicates
329   that both the mChrA and the core chromosomes have accumulated mutations in a correlated way. This
330   would support a single ancestral mChrA acquisition by the *Oryza* lineage, followed by multiple mChrA
331   losses, whereas a lack of correlation suggests independent mChrA acquisitions. By analyzing correlations
332   between genetic distances relative to Br62 instead of the magnitude of the distances, our analysis is not
333   confounded by changes in mutation rate or different strengths of purifying selection operating at the
334   mChrA and core chromosome level. We did not find any correlation in genetic distances between mChrA
335   and Br62, and core chromosomes and Br62 (**Fig 5B**). As a control, we compared genetic distances to
336   Br62 among two sets of core chromosomal regions and found a strong correlation (**Fig 5C**). Together,
337   these results favor the hypothesis that the observed mChrA distribution in the rice blast fungus lineage is
338   the result of multiple independent mChrA acquisitions.
339
340   In addition, we reconstructed the ancestral states of mChrA presence or absence along the clonal rice
341   blast fungus phylogeny and found evidence for nine independent horizontal mChrA acquisitions. Using a
342   time-scaled phylogeny, we could time these events to have occurred within the past three centuries (**Fig
343   5D**).
344
345   In summary, we provide compelling evidence supporting the scenario of multiple horizontal mChrA
346   transfers involving members of the *Eleusine* and *Oryza* blast fungus lineages. A minimum of nine
347   independent mChrA acquisitions and multiple independent losses occurred across clonal rice blast fungus
348   lineages over the past three centuries.

Fig 5. Multiple mChrA transfers occurred in clonal rice blast fungus lineages. A. *D*-statistics. Lines depict 99% confidence intervals and the red dot the estimated *D* value. Lines not encompassing *D*=0 are gray and the rest black. Jack-knife blocks were five million base pairs long. **B.** Hamming distances between mChrA and random core chromosomal regions of rice blast fungus isolates compared to Br62. **C.** Genetic distances between two sets of random core chromosomal regions in rice blast fungus isolates compared to Br62. **D.** Ancestral states of mChrA presence or absence along the clonal rice blast fungus phylogeny. Thick lines indicate mChrA is present. Branches are color-coded by lineage. The SA05-43 isolate from the *Setaria* blast fungus lineage was chosen as an outgroup. Branches with evidence for horizontal mChrA acquisition are indicated by a red diamond, the branch where there is evidence for sexual transfer or ILS is indicated by a yellow diamond.

Discussion

Crop disease pandemics are frequently caused by clonal lineages of plant pathogens that reproduce asexually. The mechanisms enabling these clonal pathogens to adapt to their hosts, despite their limited genetic variation, remain an area of active research. In our study, we demonstrate that mini-chromosomes (mChr) serve as a source of genetic variation for asexual clonal pathogens. We observed horizontal mini-chromosome transfer occurred in field isolates belonging to clonal populations of the rice blast fungus *M. oryzae*. Our findings demonstrate horizontal acquisition of a 1.2Mb supernumerary mChr by clonal rice blast isolates from a genetically distinct lineage infecting *Eleusine indica*, a wild grass species. We identified a minimum of nine independent horizontal mChr acquisitions over the past three centuries. This establishes horizontal mChr transfer as a process facilitating genetic exchange between host-associated blast fungus lineages in the field. We propose that blast fungus populations infecting wild grasses serve as genetic reservoirs for clonal populations infecting cultivated crops. Horizontal acquisition of mChr by

372   clonal blast fungus isolates appears to increase their genetic diversity, driving genome evolution and
373   potentially aiding in its adaptability.

375   The genetic mechanisms underlying horizontal minichromosome (mChr) transfer in clonal fungus isolates
376   are intriguing. Under laboratory conditions, horizontal transfer of mChr between fungal isolates has been
377   facilitated through methods such as protoplast fusion (Akagi et al. 2009) or co-culturing (Masel et al. 1996;
378   He et al. 1998; Ma et al. 2010; Vlaardingerbroek et al. 2016; van Dam et al. 2017). Underlying these mChr
379   transfers is parasexual recombination (Soanes and Richards 2014; Vlaardingerbroek et al. 2016). Here,
380   cells from different individuals fuse via anastomosis, forming heterokaryons (Roca et al. 2003; Roca et al.
381   2005; Ishikawa et al. 2010; Vangalis et al. 2021). These heterokaryons can become unstable polyploid cells,
382   undergoing chromosome reassortment during mitosis (Mela et al. 2020). In the case of *Magnaporthe* spp.
383   parasexual crosses do not exhibit heterokaryon incompatibility and are therefore viable (Crawford et al.
384   1986). This mechanism has been suggested as a source of genetic variation in the rice blast fungus,
385   potentially occurring under field conditions (Zeigler et al. 1997; Noguchi et al. 2006; Tsujimoto Noguchi
386   2011; Monsur and Kusaba 2018). Here, we found robust evidence that horizontal mChr transfer occurs
387   under field conditions, a process probably parasexual in nature.

389   Parasexuality offers fungi an alternative route to enhancing genetic diversity, while maintaining relative
390   genomic stability and avoiding the complexities of sexual reproduction, including pre-mating barriers like
391   reproductive timing and post-mating issues such as hybrid incompatibilities (Roper et al. 2011;
392   Stukenbrock 2013). Recently, it was proposed that chromosome reassortment during parasexual
393   recombination may not be entirely random (Habig et al. 2023). Here, it was suggested that some mChr
394   are preferentially transferred or tend to resist degradation compared to others, resembling the behavior
395   of selfish genetic elements (Ahmad and Martins 2019). This phenomenon could be attributed to distinct
396   chromatin conformations of the mChr. Future research will investigate whether mChrA carries chromatin
397   remodeling elements that could enable its horizontal transfer or shield it from degradation, potentially
398   elucidating the relatively frequent horizontal transfer events observed across the rice blast fungus lineage.
399   Moreover, to better understand the impact of horizontal mChr transfer on *M. oryzae* evolution, it will be
400   crucial to study how frequent and diverse these events are in field populations.

402   Not all instances of inter-lineage transfer events of the mChrA sequence seem to be the product of
403   parasexually-mediated horizontal transfer. Hybridization through sexual mating is a major player shaping
404   the evolution of fungal plant pathogens, bringing forth a myriad of novel genetic combinations for selection
405   pressures to act on (Stukenbrock 2016). In *M. oryzae*, there is evidence of sexual mating occurring both
406   within and between specific host-associated blast fungus lineages, occasionally facilitating host jumps
407   (Gladieux, Ravel, et al. 2018). In our study, one clonal rice blast fungus isolate, BR0026, exhibited genome-
408   wide introgression signals with *Eleusine* isolate Br62. One plausible hypothesis is that the introgression
409   signals observed in BR0026 may reflect ancient sexual reproduction events involving an isolate from the
410   *Eleusine* lineage. Given that these two isolates were collected in South America, it is possible that sympatry
411   in this region led to sexual reproduction between members of the rice and *Eleusine* lineages.

413   In addition to isolates belonging to the *Eleusine* and *Oryza* blast fungus lineages, isolates belonging to the
414   *Triticum* and *Lolium* lineages also carry mChrA-like sequences. It remains to be determined whether these
415   were obtained via horizontal transfer or sexual reproduction. The absence of genetic discordance between

416   the core chromosomes and mChrA in these isolates supports sexual reproduction. In addition, substantial
417   admixture has been observed among members of the *Triticum* and *Lolium* lineages (Gladieux, Ravel, et al.
418   2018), suggesting that sexual reproduction may be the route through which mChrA-like sequences were
419   acquired.
420
421   Our study on the prevalence of horizontal gene exchange within local populations underscores the
422   importance of accounting for ecological factors, especially in fungi that tend to specialize in specific hosts.
423   Although our global comprehension of blast fungus populations has expanded, the detailed study of local
424   populations, particularly those that include isolates from both wild and cultivated hosts, remain scarce
425   (Cruz and Valent 2017; Barragan et al. 2022). One question to address will be how horizontal gene
426   exchange through parasexuality is enabled in natural environments. In the case of the blast fungus, one
427   factor offering an avenue for genetic interchange may be the absence of strict host-specialization (Gladieux,
428   Condon, et al. 2018). Laboratory studies have shown that hosts like barley and common millet are
429   susceptible to genetically distinct blast fungus lineages (Kato et al. 2000; Hyon et al. 2012; Chung et al.
430   2020). In the field, some cases of cross-infection have been reported, but the extent to which these occur
431   in local populations is unknown (Gladieux, Condon, et al. 2018). Such susceptible hosts could serve as
432   hubs for genetic exchanges, potentially contributing to horizontal mChr transfers between isolates from
433   different lineages. Moreover, being a facultative biotroph, the blast fungus possesses the ability to thrive
434   on both living plants and saprophytically on decaying plant matter. This broadens the window for possible
435   genetic interactions, as the pathogen does not require synchronous growth within the same living hosts
436   for this to occur. Understanding gene flow within local blast fungus populations through the study of
437   horizontal gene transfer and other mechanisms, is vital for developing effective disease management
438   strategies. For example, identifying frequent horizontal gene exchange between isolates infecting specific
439   hosts could lead to targeted measures such as strategic weeding or focused fungicide application.
440
441   One persistent challenge in pinpointing elements of the accessory genome, such as mChr, has been the
442   biases arising from aligning sequencing reads to a single reference genome. In past comparative genomic
443   approaches, mChrA went unnoticed, as we aligned isolates carrying this sequence to the MG08 reference
444   genome from isolate 70-15, which lacks the mChrA sequence. Leveraging pan-genomes, which are
445   continuously gaining traction across the fungal kingdom (Badet and Croll 2020) or *de novo* assemblies using
446   short read data (Potgieter et al. 2020), coupled with reference-independent genetic clustering approaches
447   like k-mer (Zielezinski et al. 2017; Aylward et al. 2023) or read-based (Dylus et al. 2024) techniques,
448   promises more accurate identification of mChr and of horizontally introgressed regions. The latter could
449   be detected by first identifying mChr and other accessory genomic elements, and then comparing them
450   with the core genome. Studies of this nature have recently detected cases of horizontal introgression in
451   other fungal pathogens (Moolhuijzen et al. 2022; Petersen et al. 2023). In addition to these approaches,
452   the integration of artificial intelligence to distinguish between core chromosomes and mChr using short-
453   read sequencing data presents a timely and innovative approach (Gyawali et al. 2023). The successful
454   implementation of such methodologies will not only facilitate the large-scale identification of candidate
455   mChr regions across isolates, but also help establish whether these regions are preferentially involved in
456   horizontal transfer events.
457
458   The horizontal transfer of mChrA from a blast fungus lineage that infects the wild grass *Eleusine indica* to
459   clonal rice blast fungus lineages underscores the intricate ecological interactions involved. Wild grasses

460   can act as potential genetic reservoirs, echoing the dynamics observed in zoonotic diseases where
461   pathogens jump between wild animals and humans (Rahman et al. 2020). This analogy between the plant
462   and animal realms highlights the significance of wild species as reservoirs of pathogens and suggests the
463   possibility of genetic transfers. However, surveys on blast disease often focus on cultivated crops,
464   neglecting wild hosts (Barragan et al. 2022). Therefore, enhanced awareness and surveillance of gene flow
465   dynamics in local blast fungus populations are necessary. This should include investigations into the role
466   of wild grasses as genetic conduits, similar to the concept of zoonoses. Such understanding is crucial for
467   the early identification and prevention of genetic transfers that could initiate new disease outbreaks or
468   intensify existing ones.
469
470   **Conclusion**
471   Clonal isolates of the blast fungus are a significant agricultural concern due to their central role in causing
472   crop disease pandemics. Key to tackling this issue is understanding how genetically uniform populations
473   adapt to novel hosts. Our research has revealed that supernumerary mini-chromosomes undergo
474   horizontal transfer in natural field conditions. Notably, we found that mChrA has been transferred
475   horizontally on multiple independent occasions involving isolates from a lineage of blast fungus affecting a
476   wild grass and clonal lineages infecting rice. This finding sheds light on the role of horizontal mini-
477   chromosome transfer in driving the genome evolution of clonal blast fungus populations, potentially aiding
478   in host adaptation. Isolates originating from wild grasses may act as reservoirs of genetic diversity (**Fig 6**).
479   These insights underscore the importance of disease surveillance that encompasses both agricultural crops
480   and adjacent wild grass species.
481
482   **Model**
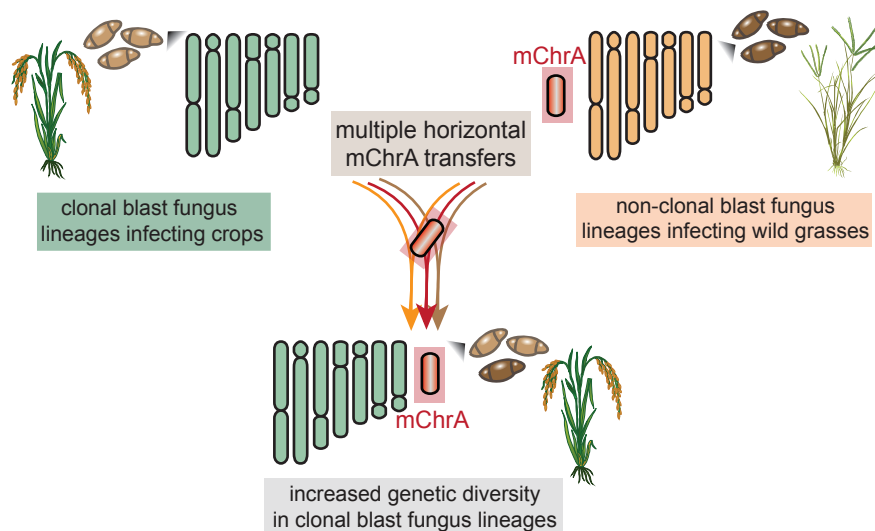
Fig 6. Horizontal mini-chromosome transfers from blast fungus lineages infecting wild grasses drive genome evolution of clonal lineages infecting crops. The recurrent acquisition of mChrA from wild grass-infecting blast fungus lineages by clonal rice blast fungus lineages enhances their evolutionary adaptability and capacity to respond to changing environments and hosts. The coexistence of infected crops and wild hosts facilitates this genetic exchange, posing a challenge to the management of crop disease pandemics.

490   **Materials and Methods**
491   **Blast fungus growth conditions**

492   Blast fungus isolates were grown from filter paper stocks by placing these on complete medium (CM) for
493   7-14 days in a growth chamber at 24°C with a 12 hour light period to induce growth of mycelium and
494   sporulation. For liquid cultures, 8-10 small blocks of mycelium (ca. 0.5 x 0.5cm) were cut out of the edge
495   of fully grown colonies with a sterile spatula, transferred into 150ml of liquid CM medium in a 250ml
496   Erlenmeyer flask and incubated on a rotary shaker at 120 rpm and 24°C for 2-3 days.

497

498   **Visualization of worldwide blast fungus distribution**
499   Maps showing the geographical locations of the studied blast fungus isolates were plotted with the R-
500   package ggmap (v3.0) (Kahle and Wickham 2013). In the case of the San Andrea isolate, no exact collection
501   coordinates were available, so the location of the San Andrea Chapel in Ravenna, in Italy's Po Valley, the
502   region where most other samples were collected from, was chosen.

503

504   **Whole-genome and mini-chromosome sequencing and genome assembly**
505   Whole-genome sequencing and assembly of nine Italian blast fungus isolates, including AG006, is described
506   in (Win et al. 2020). Briefly, these isolates were sequenced using the PromethION sequencing platform
507   (Oxford Nanopore Technologies, Oxford, UK) and assembled into contigs using Canu (Koren et al. 2017).
508   Assemblies were then polished with Illumina short reads using Pilon (Walker et al. 2014) and Racon (Vaser
509   et al. 2017) and their completeness assessed using BUSCO (Simão et al. 2015), with a 97.7-98.8%
510   completeness score taking the ascomycota_odb10 database as input (Win et al. 2020). Mini-chromosome
511   isolation sequencing (MCIS) of these isolates was performed as described in (Langner et al. 2019; Langner
512   et al. 2021). In short, mini-chromosomes (mChr) were separated from core chromosomes using CHEF
513   gel electrophoresis. DNA was eluted from gel plugs and sequencing libraries were prepared using a
514   modified version (custom barcodes) of the Nextera Flex library preparation kit (Illumina). Sequencing of
515   mini-chromosomal DNA libraries was carried out on a NextSeq500 system (Illumina). For whole-genome
516   sequencing and de *novo* assembly generation of the Br62 isolate, high molecular weight DNA was extracted
517   following (Jones et al. 2021). Sequencing runs were then performed by Future Genomics Technologies
518   (Leiden, The Netherlands) using the PromethION sequencing platform (Oxford Nanopore Technologies,
519   Oxford, UK). Long reads were assembled into contigs and corrected using Flye (v2.9-b17680)
520   (Kolmogorov et al. 2019) and polished with long reads using Medaka (v1.7.2)
521   (https://github.com/nanoporetech/medaka), and using Illumina short reads (San Diego, USA) through two
522   consecutive iterations of Pilon (v1.23) (Walker et al. 2014). The resulting assembly was of high quality and
523   contiguity, with a BUSCO (Simão et al. 2015) completeness score of 97.4% using the ascomycota_odb10
524   database and resulting in ten contigs (**Table S10**).

525

526   **Identification of mini-chromosomes in whole-genome assemblies**
527   MCIS read quality was assessed using fastQC (Andrews 2010). Low quality and adapter sequences were
528   removed using trimmomatic (Bolger et al. 2014). mChr reads were mapped to whole-genome assemblies
529   of each strain using BWA-mem (Li 2013) with default parameters. Reads with multiple mappings (mapping
530   quality = 0) and secondary alignments were removed using samtools (Danecek et al. 2021). MCIS read
531   coverage was calculated in 1kb sliding windows with a step size of 500bp using bedtools (Quinlan and Hall
532   2010). The depth of unambiguously mapping reads was plotted using the R package circlize (Gu et al.
533   2014). To estimate the repeat content across core and mChr in the nine Italian rice blast isolates, we
534   annotated these using RepeatMasker (http://www.repeatmasker.org/). The input repeat library consisted
535   of the RepBase repeat library for fungi (https://www.girinst.org/repbase/), and repeat libraries from

536 (Chiapello et al. 2015; Peng et al. 2019). For <2Mb contigs repeat content was plotted across 100kb sliding
537 windows and a step size of 50kb, while for >2Mb contigs 10kb windows with a 5kb step size were chosen.
538
539 ### Whole-genome and mini-chromosome alignments and telomere identification
540 Whole genome and contig-specific alignments between *M. oryzae* isolates were generated using the
541 nucmer function of MUMMER4 (Marçais et al. 2018). Alignments of a minimum length of 10kb (-l 10000)
542 and >80% percent identity (-i 80) were chosen to retrieve contiguous alignments. Alignment coordinates
543 were extracted and whole genome alignments were plotted using the circlize package (Gu et al. 2014).
544 Alignments between individual contigs were visualized with the karyoploteR package (Gel and Serra 2017).
545 We visually inspected mChr contigs for the presence of (CCCTAA/TTAGGG)n canonical telomeric
546 repeats (Cevernak et al. 2021).
547
548 ### Genetic analysis of blast fungus isolates: mapping and variant calling
549 Illumina short reads of 413 *M. oryzae* and *M. grisea* isolates infecting different host plants (**Table S6**)
550 were trimmed using AdapterRemoval (v2.3.1) (Schubert et al. 2016) and then mapped to the AG006
551 reference genome (Win et al. 2020) using bwa-mem (v0.7.17) (Li 2013) with default parameters. Variant
552 identification was performed using GATK (v4.1.4.0) (McKenna et al. 2010). High-quality SNPs were filtered
553 based on the Quality-by-Depth (QD) parameter using GATK's VariantFiltration. Only biallelic SNPs within
554 one standard deviation of the median value of QD scores across all SNPs were kept (Latorre et al. 2022).
555 To study the phylogenetic relationship between isolates belonging to the rice blast fungus lineage, we
556 subsetted 274 isolates belonging to this lineage (isolates BF5 and BTAr-A1 were removed due to them
557 being outliers in the rice blast fungus phylogeny) and kept informative SNPs with no missing data using
558 VCFtools (v0.1.14). From this dataset, we created a NeighborNet using Splitstree (Huson and Bryant
559 2006). We repeated this process for members of the *Oryza* clonal lineage II only, and constructed a
560 Maximum-Likelihood (ML) tree using MEGA (v10.2.4) (Kumar et al. 2018), with 100 bootstraps (see data
561 availability). We repeated the same process for the analysis of all 413 isolates shown in Fig 1 (**Table S6**).
562 Here, two isolates were removed due to the high amount of missing sites (FR13 and 98-06). Based on
563 these SNPs, we created a NJ tree using MEGA (v10.2.4) (Kumar et al. 2018), with 100 bootstraps (see
564 data availability). Isolates deemed as mChrA carriers were highlighted using iTol (Letunic and Bork 2021).
565 To assess for potential discordance in genetic clustering of the core genome and mChrA, we subsetted
566 isolates carrying mChrA (n=126). For both the core genome and mChrA, only SNPs with a maximum of
567 10% missing data were kept (--max-missing 0.9) using VCFtools (v0.1.11). NJ trees were constructed using
568 IQtree (v2.03) using fast mode (see data availability). SNP-based Principal Component Analyses (PCA)
569 were estimated using the --pca function of PLINK2 (Chang et al. 2015). These were visualized using the R
570 package ggplot2 (v3.4.4, see data availability) (Wickham 2009). To determine the likelihood of the
571 observed genetic discordance being observed by chance, 100 random 1.2Mb regions across the core
572 genome in these 126 isolates were subsetted using a custom python script (see data availability), and NJ
573 trees were computed using IQTree (v2.03) with the fast mode. The number of times each lineage was
574 monophyletic was estimated using a provided custom python script (see data availability). To evaluate
575 genetic differentiation between members of the *Eleusine* and *Oryza* lineages carrying the mChrA sequence,
576 the fixation index (F_{ST}) based on genome-wide SNPs was calculated. Rice blast isolates carrying mChrA
577 (n=32) were compared to the two *Eleusine* isolates carrying mChrA, Br62 and B51, using only SNPs with
578 no missing data. Weighted F_{ST} using 5kb window sizes and 500bp step sizes (--fst-window-size 5000 --fst-
579 step-size 500) was calculated using VCFtools (v0.1.14).

mChrC and mChrA breadth of coverage calculations and mChrA-carrier assignment

To investigate the distribution of the mChrC and mChrA sequence across 413 *M. oryzae* and *M. grisea* isolates, we first calculated the genome-wide breadth of coverage, defined as the percentage of sequence covered by reads from a particular isolate which mapped to the AG006 reference (**Table S6**). To do this, we estimated breadth of coverage per contig using samtools depth (v1.19) (Danecek et al. 2021), and then created a weighted average taking into account contig length. We assessed breadth of coverage for mChrC (AG006_Contig03) and mChrA (AG006_Contig10) across all isolates and then normalized these values by the isolate's genome-wide breadth of coverage value (**Table S6**). To determine whether an isolate carried the mChrA sequence or not, we performed clustering using a gaussian mixture model (GMM) and estimated the Bayesian Information Criterion (BIC) value for 1-10 clusters using the R-package mclust (v.6.0.0, see data availability) (Scrucca et al. 2023). Using this same package, we also estimated the uncertainty index for mChrA presence (n=126) or absence (n=287) assignment for each isolate (**Table S9**).

Identification of mChrA in *Eleusine* isolate Br62 and mChrA loss Br62-

M. oryzae isolate Br62, belonging to the *Eleusine* lineage, initially carried a single mChr identical in size to mChrA (1.2Mb). To confirm the identity of this mChr, we subcultured Br62 twice via serial passage on Complete Growth Medium (CM), resulting in the loss of mChr as confirmed through CHEF gel electrophoresis. We then sequenced the genome of Br62 without the 1.2Mb mChr (referred to as Br62-) using Illumina short-reads and compared it to the complete Br62 genome sequences. Mapping depth per contig was calculated using the samtools depth function (Danecek et al. 2021). Depths were consistent between Br62 and Br62- except for Contig07, corresponding to mChrA, where Br62- displayed a near-zero read depth. Additionally, repeat content analysis for the Br62 genome, using the same parameters as for the Italian rice blast fungus isolates.

Differentiation between horizontal mChrA transfer from introgression via sexual mating

To differentiate between horizontal mChr transfer or sexual mating we assessed patterns of allele sharing and calculated *D* statistics (Green et al. 2010; Durand et al. 2011) using popstats (Skoglund et al. 2015) as well as using the custom python script *Dstat.py* (see data availability). We removed the mChrA sequence from the *Eleusine* and *Oryza* mChrA carriers and set the *M. grisea* isolate Dig41 as an outgroup, resulting in the following 4-taxa configuration: (Dig41, Br62; *Oryza* +mChrA, *Oryza* -mChrA). The selection of the non-carrier samples (-mChrA) was random and contingent on their phylogenetic proximity to the tested mChrA carrier (+mChrA) isolate (**Table S11**). In the case of +mChrA isolate AG006, we performed comparisons against 13 different *Oryza* -mChrA isolates, selected throughout along the different clades of the clonal lineage II. As a control, we also tested the 4-taxa configuration: (Dig41, Br62; *Oryza* +mChrA, *Oryza* +mChrA). The tested isolates were selected based on them having phylogenetic proximity. Complementary to this, we included a second control using the 4-taxa configuration: (Dig41, Br62; *Oryza* -mChrA, *Oryza* -mChrA). The testing pair of isolates were chosen randomly and contingent on being part of the same genetic subgroup of the rice blast fungus lineage. In all tested configurations, we only compared rice blast fungus isolates belonging to the same subgroup, to avoid potential unequal drift accumulated between members of different clonal lineages from impacting the analysis. For each configuration we calculated the 99% confidence interval. *D* values were estimated for jack-knife blocks 5 and 10 million base pairs in length (**Table S11**).

Differentiating between a single and multiple horizontal mChrA transfer events

To differentiate between a single ancestral gain of mChrA followed by independent losses, and independent mChrA gains. We measured Hamming distances between mChrA in all *Oryza* isolates carrying this sequence (n=32) and *Eleusine* isolate Br62, and Hamming distances across random core chromosomal regions (the size of mChrA, 1.2Mb) and Br62 using bcftools (v.1.11) (Danecek et al. 2021), (see data availability). We then assessed if there is correlation between the two hamming distances. Both Pearson's correlation coefficient and its *p*-value were estimated. As a control, we compared average Hamming distances between two sets of core chromosomal regions to Br62 and again calculated Pearson's correlation coefficient and its *p*-value.

Dating of horizontal mChrA transfer Events Across Clonal Rice Blast Fungus Lineages

In order to infer the dating times of horizontal acquisition of the mChrA sequence in the ancestral nodes of the rice blast fungus phylogeny, we performed a bayesian-based dated phylogeny incorporating the isolate collection dates (**Table S6**) using BEAST2 (Bouckaert et al. 2014). We selected the Hasegawa-Kishino-Yano (HKY) nucleotide substitution model. The collection years of the blast fungus isolates served as prior information, providing expected units for the estimated evolutionary rate (substitutions/site/year). In Bayesian analysis, we utilized a log-normal distribution with a mean in real space set at 7.5E-8, based on previous estimations (Latorre et al. 2022). To minimize the effect of demographic assumptions, we chose a Coalescent Extended Bayesian Skyline as a tree prior (Drummond et al. 2005). Isolates without a known collection date were removed from this analysis, and only individuals belonging to rice blast clonal lineages were used to rule out recombination. We ran six independent chains, each spanning a length of 20 million iterations using the CIPRES infrastructure (Miller et al. 2010). To ascertain the ancestral states of presence or absence of the mChrA sequence throughout the rice blast fungus phylogeny, we used the inferred mChrA presence/absence information based on breadth of coverage analyses (**Table S9**). This was done for all rice blast fungus isolates, as well as for the SA05-43 isolate which belongs to the *Setaria* blast fungus lineage, which was set as an outgroup. These values, which were input as discrete states (mChrA = yes/no), were parameterized in a "mugration" analysis, which was implemented in Treetime (v.0.9.0) (Sagulenko et al. 2018) ML-tree as input, generated using IQtree (v2.03) (Minh et al. 2020).

Textual enhancement

The articulation of text within this manuscript was assisted by the machine learning model ChatGPT-4.

668   101077853 (to TL), the Royal Society grant RSWF\R1\191011 and a Philip Leverhulme Prize from The
669   Leverhulme Trust (to HAB), the EPSRC Doctoral Training Partnerships (DTP), and a Walter Benjamin
670   Postdoctoral Fellowship from the German Research Council (to ACB). The funders had no role in study
671   design, data collection and analysis, decision to publish, or preparation of the manuscript.
672

Data availability

674   The authors confirm that all data underlying the findings are fully available without restriction. Files and
675   code to perform the analyses described and to generate the plots presented are available as Supplementary
676   Files, and in the git repository: https://github.com/smlatorreo/mChr_Moryzae (Latorre 2024). Sequencing
677   reads were deposited in the European Nucleotide Archive (ENA) under study accession number
678   PRJEB6623 (mini-chromosome sequences from Italian rice blast isolates) and PRJEB67435 (Br62-
679   sequencing). In addition, the Br62 whole-genome assembly is available under GenBank accession number
680   PRJEB66723.
681

Author Contributions

683   **Conceptualization:** ACB, SML, HAB, SK, TL.
684   **Formal analysis:** ACB, SML, AM, AH, JW, TL.
685   **Investigation:** ACB, SML, AM, AH, JW, YS, TL.
686   **Visualization:** ACB, SML, AM, TL.
687   **Coding:** ACB, SML, AM, TL.
688   **Supervision:** HAB, SK.
689   **Writing – original draft:** ACB.
690   **Writing – review & editing:** ACB, SML, HAB, SK and TL with contributions from all authors.
691   **Project administration:** ACB, SK.
692   **Funding acquisition:** ACB, HAB, SK, TL.
693

694   **Competing interests**. The authors have declared that no competing interests exist.
695

References

697   Ahmad SF, Martins C. 2019. The Modern View of B Chromosomes Under the Impact of High Scale
698   Omics Analyses. *Cells* [Internet] 8. Available from: http://dx.doi.org/10.3390/cells8020156

699   Akagi Y, Akamatsu H, Otani H, Kodama M. 2009. Horizontal chromosome transfer, a mechanism for the
700   evolution and differentiation of a plant-pathogenic fungus. *Eukaryot. Cell* 8:1732–1738.

701   Andrews S. 2010. FastQC: a quality control tool for high throughput sequence data.

702   Asuke S, Horie A, Komatsu K, Mori R, Vy TTP, Inoue Y, Jiang Y, Tatematsu Y, Shimizu M, Tosa Y. 2023.
703   Loss of PWT7 located on a supernumerary chromosome is associated with parasitic specialization
704   of Pyricularia oryzae on wheat. *Mol. Plant. Microbe. Interact.* [Internet]. Available from:
705   http://dx.doi.org/10.1094/MPMI-06-23-0078-R

706   Aylward AJ, Petrus S, Mamerto A, Hartwick NT, Michael TP. 2023. PanKmer: k-mer based and
707   reference-free pangenome analysis. *bioRxiv* [Internet]:2023.03.31.535143. Available from:
708   https://www.biorxiv.org/content/10.1101/2023.03.31.535143

709 Badet T, Croll D. 2020. The rise and fall of genes: origins and functions of plant pathogen pangenomes.
710   *Curr. Opin. Plant Biol.* 56:65–73.

711 Balesdent M-H, Fudal I, Ollivier B, Bally P, Grandaubert J, Eber F, Chèvre A-M, Leflon M, Rouxel T.
712   2013. The dispensable chromosome of Leptosphaeria maculans shelters an effector gene conferring
713   avirulence towards Brassica rapa. *New Phytol.* 198:887–898.

714 Barragan AC, Latorre SM, Mock PG, Harant A, Win J, Malmgren A, Burbano HA, Kamoun S, Langner T.
715   2022. Wild grass isolates of Magnaporthe (Syn. Pyricularia) spp. from Germany can cause blast
716   disease on cereal crops. *bioRxiv* [Internet]:2022.08.29.505667. Available from:
717   https://www.biorxiv.org/content/10.1101/2022.08.29.505667v1

718 Barragan AC, Weigel D. 2021. Plant NLR diversity: the known unknowns of pan-NLRomes. *Plant Cell*
719   33:814–831.

720 Barrett RDH, Schluter D. 2008. Adaptation from standing genetic variation. *Trends Ecol. Evol.* 23:38–44.

721 Barrett SCH. 2010. Understanding plant reproductive diversity. *Philos. Trans. R. Soc. Lond. B Biol. Sci.*
722   365:99–109.

723 Bertazzoni S, Williams AH, Jones DA, Syme RA, Tan K-C, Hane JK. 2018. Accessories Make the Outfit:
724   Accessory Chromosomes and Other Dispensable DNA Regions in Plant-Pathogenic Fungi. *Mol.*
725   *Plant. Microbe. Interact.* 31:779–788.

726 Bhadauria V, MacLachlan R, Pozniak C, Cohen-Skalie A, Li L, Halliday J, Banniza S. 2019. Genetic map-
727   guided genome assembly reveals a virulence-governing minichromosome in the lentil anthracnose
728   pathogen Colletotrichum lentis. *New Phytol.* 221:431–445.

729 Bolger AM, Lohse M, Usadel B. 2014. Trimmomatic: a flexible trimmer for Illumina sequence data.
730   *Bioinformatics* 30:2114–2120.

731 Bouckaert R, Heled J, Kühnert D, Vaughan T, Wu C-H, Xie D, Suchard MA, Rambaut A, Drummond AJ.
732   2014. BEAST 2: a software platform for Bayesian evolutionary analysis. *PLoS Comput. Biol.*
733   10:e1003537.

734 Cervenak F, Sepsiova R, Nosek J, Tomaska L. 2021. Step-by-Step Evolution of Telomeres: Lessons from
735   Yeasts. *Genome Biol. Evol.* [Internet] 13. Available from: http://dx.doi.org/10.1093/gbe/evaa268

736 Chang CC, Chow CC, Tellier LC, Vattikuti S, Purcell SM, Lee JJ. 2015. Second-generation PLINK: rising
737   to the challenge of larger and richer datasets. *Gigascience* 4:7.

738 Chiapello H, Mallet L, Guérin C, Aguileta G, Amselem J, Kroj T, Ortega-Abboud E, Lebrun M-H,
739   Henrissat B, Gendrault A, et al. 2015. Deciphering Genome Content and Evolutionary Relationships
740   of Isolates from the Fungus Magnaporthe oryzae Attacking Different Host Plants. *Genome Biol. Evol.*
741   7:2896–2912.

742 Chuma I, Isobe C, Hotta Y, Ibaragi K, Futamata N, Kusaba M, Yoshida K, Terauchi R, Fujita Y,
743   Nakayashiki H, et al. 2011. Multiple translocation of the AVR-Pita effector gene among
744   chromosomes of the rice blast fungus Magnaporthe oryzae and related species. *PLoS Pathog.*
745   7:e1002147.

746 Chung H, Goh J, Han S-S, Roh J-H, Kim Y, Heu S, Shim H-K, Jeong DG, Kang IJ, Yang J-W. 2020.
747   Comparative Pathogenicity and Host Ranges of Magnaporthe oryzae and Related Species. *Plant*

748   *Pathol. J.* 36:305–313.

749   Couch BC, Fudal I, Lebrun M-H, Tharreau D, Valent B, van Kim P, Nottéghem J-L, Kohn LM. 2005.
750   Origins of host-specific populations of the blast pathogen Magnaporthe oryzae in crop
751   domestication with subsequent expansion of pandemic clones on rice and weeds of rice. *Genetics*
752   170:613–630.

753   Covert SF. 1998. Supernumerary chromosomes in filamentous fungi. *Curr. Genet.* 33:311–319.

754   Crawford MS, Chumley FG, Weaver CG, Valent B. 1986. Characterization of the Heterokaryotic and
755   Vegetative Diploid Phases of MAGNAPORTHE GRISEA. *Genetics* 114:1111–1129.

756   Croll D, McDonald BA. 2012. The accessory genome as a cradle for adaptive evolution in pathogens.
757   *PLoS Pathog.* 8:e1002608.

758   Cruz CD, Valent B. 2017. Wheat blast disease: danger on the move. *Trop. Plant Pathol.* 42:210–222.

759   van Dam P, Fokkens L, Ayukawa Y, van der Gragt M, ter Horst A, Brankovics B, Houterman PM, Arie T,
760   Rep M. 2017. A mobile pathogenicity chromosome in Fusarium oxysporum for infection of multiple
761   cucurbit species. *Sci. Rep.* 7:1–15.

762   Danecek P, Bonfield JK, Liddle J, Marshall J, Ohan V, Pollard MO, Whitwham A, Keane T, McCarthy SA,
763   Davies RM, et al. 2021. Twelve years of SAMtools and BCFtools. *Gigascience* [Internet] 10. Available
764   from: http://dx.doi.org/10.1093/gigascience/giab008

765   Dong S, Raffaele S, Kamoun S. 2015. The two-speed genomes of filamentous pathogens: waltz with
766   plants. *Curr. Opin. Genet. Dev.* 35:57–65.

767   Drenth A, McTaggart AR, Wingfield BD. 2019. Fungal clones win the battle, but recombination wins the
768   war. *IMA Fungus* 10:18.

769   Drummond AJ, Rambaut A, Shapiro B, Pybus OG. 2005. Bayesian coalescent inference of past
770   population dynamics from molecular sequences. *Mol. Biol. Evol.* 22:1185–1192.

771   Durand EY, Patterson N, Reich D, Slatkin M. 2011. Testing for ancient admixture between closely
772   related populations. *Mol. Biol. Evol.* 28:2239–2252.

773   Dylus D, Altenhoff A, Majidian S, Sedlazeck FJ, Dessimoz C. 2024. Inference of phylogenetic trees
774   directly from raw sequencing reads using Read2Tree. *Nat. Biotechnol.* 42:139–147.

775   Fitzpatrick DA. 2012. Horizontal gene transfer in fungi. *FEMS Microbiol. Lett.* 329:1–8.

776   Gabaldón T. 2020. Patterns and impacts of nonvertical evolution in eukaryotes: a paradigm shift. *Ann. N.*
777   *Y. Acad. Sci.* 1476:78–92.

778   Gel B, Serra E. 2017. karyoploteR: an R/Bioconductor package to plot customizable genomes displaying
779   arbitrary data. *Bioinformatics* 33:3088–3090.

780   Gladieux P, Condon B, Ravel S, Soanes D, Maciel JLN, Nhani A Jr, Chen L, Terauchi R, Lebrun M-H,
781   Tharreau D, et al. 2018. Gene Flow between Divergent Cereal- and Grass-Specific Lineages of the
782   Rice Blast Fungus Magnaporthe oryzae. *MBio* [Internet] 9. Available from:
783   http://dx.doi.org/10.1128/mBio.01219-17

784   Gladieux P, Ravel S, Rieux A, Cros-Arteil S, Adreit H, Milazzo J, Thierry M, Fournier E, Terauchi R,
785   Tharreau D. 2018. Coexistence of Multiple Endemic and Pandemic Lineages of the Rice Blast
786   Pathogen. *MBio* [Internet] 9. Available from: http://dx.doi.org/10.1128/mBio.01806-17

787   Green RE, Krause J, Briggs AW, Maricic T, Stenzel U, Kircher M, Patterson N, Li H, Zhai W, Fritz MH-
788   Y, et al. 2010. A draft sequence of the Neandertal genome. *Science* 328:710–722.

789   Gu Z, Gu L, Eils R, Schlesner M, Brors B. 2014. circlize Implements and enhances circular visualization in
790   R. *Bioinformatics* 30:2811–2812.

791   Gyawali N, Hao Y, Lin G, Huang J, Bika R, Daza LC, Zheng H, Cruppe G, Caragea D, Cook D, et al.
792   2023. Using recurrent neural networks to detect supernumerary chromosomes in fungal strains
793   causing blast diseases. *bioRxiv* [Internet]:2023.09.17.558148. Available from:
794   https://www.biorxiv.org/content/10.1101/2023.09.17.558148v1

795   Habig M, Grasse AV, Mueller J, Stukenbrock EH, Leitner H, Cremer S. 2023. Frequent horizontal
796   chromosome transfer between asexual fungal insect pathogens. *bioRxiv*
797   [Internet]:2023.09.18.558174. Available from:
798   https://www.biorxiv.org/content/10.1101/2023.09.18.558174v1

799   Habig M, Quade J, Stukenbrock EH. 2017. Forward Genetics Approach Reveals Host Genotype-
800   Dependent Importance of Accessory Chromosomes in the Fungal Wheat Pathogen Zymoseptoria
801   tritici. *MBio* [Internet] 8. Available from: http://dx.doi.org/10.1128/mBio.01919-17

802   Han Y, Liu X, Benny U, Kistler HC, VanEtten HD. 2001. Genes determining pathogenicity to pea are
803   clustered on a supernumerary chromosome in the fungal plant pathogen Nectria haematococca.
804   *Plant J.* 25:305–314.

805   He C, Rusu AG, Poplawski AM, Irwin JA, Manners JM. 1998. Transfer of a supernumerary chromosome
806   between vegetatively incompatible biotypes of the fungus Colletotrichum gloeosporioides. *Genetics*
807   150:1459–1466.

808   Henry PM, Pincot DDA, Jenner BN, Borrero C, Aviles M, Nam M-H, Epstein L, Knapp SJ, Gordon TR.
809   2021. Horizontal chromosome transfer and independent evolution drive diversification in Fusarium
810   oxysporum f. sp. fragariae. *New Phytol.* 230:327–340.

811   Huang J, Liu S, Cook DE. 2023. Dynamic Genomes - Mechanisms and consequences of genomic diversity
812   impacting plant-fungal interactions. *Physiol. Mol. Plant Pathol.* 125:102006.

813   Huson DH, Bryant D. 2006. Application of phylogenetic networks in evolutionary studies. *Mol. Biol. Evol.*
814   23:254–267.

815   Hyon G-S, Nga NTT, Chuma I, Inoue Y, Asano H, Murata N, Kusaba M, Tosa Y. 2012. Characterization
816   of interactions between barley and various host-specific subgroups of Magnaporthe oryzae and M.
817   grisea. *J. Gen. Plant Pathol.* 78:237–246.

818   Ishikawa FH, Barcelos QL, Alves E, Camargo OA Jr, de Souza EA. 2010. Symptoms and prepenetration
819   events associated with the infection of common bean by the anamorph and teleomorph
820   ofGlomerella cingulataf.Sp.Phaseoli. *J. Phytopathol.* 158:270–277.

821   Islam T, Ansary MWR, Rahman MM. 2023. Magnaporthe oryzae and Its Pathotypes: A Potential Plant
822   Pandemic Threat to Global Food Security. In: Scott B, Mesarich C, editors. Plant Relationships:

823   Fungal-Plant Interactions. Cham: Springer International Publishing. p. 425–462.

824   Jones A, Torkel C, Stanley D, Nasim J, Borevitz J, Schwessinger B. 2021. High-molecular weight DNA
825   extraction, clean-up and size selection for long-read sequencing. *PLoS One* 16:e0253830.

826   Kahle D, Wickham H. 2013. ggmap: Spatial Visualization with ggplot2. *R J.* 5:144–161.

827   Kato H, Yamamoto M, Yamaguchi-Ozaki T, Kadouchi H, Iwamoto Y, Nakayashiki H, Tosa Y, Mayama S,
828   Mori N. 2000. Pathogenicity, Mating Ability and DNA Restriction Fragment Length Polymorphisms
829   of Pyricularia Populations Isolated from Gramineae, Bambusideae and Zingiberaceae Plants. *J. Gen.*
830   *Plant Pathol.* 66:30–47.

831   Kistler CH. 1996. Mutants ofNectria haematococcaCreated by a site-directed chromosome breakage
832   are greatly reduced in virulence toward pea. *Mol. Plant. Microbe. Interact.* 9:804.

833   Kobayashi N, Dang TA, Kieu PTM, Gómez Luciano LB, Van Ba V, Izumitsu K, Shimizu M, Ikeda K-I, Li
834   W-H, Nakayashiki H. 2023. Horizontally transferred DNA in the genome of the fungus Pyricularia
835   oryzae is associated with repressive histone modifications. *Mol. Biol. Evol.* [Internet]. Available from:
836   http://dx.doi.org/10.1093/molbev/msad186

837   Kolmogorov M, Yuan J, Lin Y, Pevzner PA. 2019. Assembly of long, error-prone reads using repeat
838   graphs. *Nat. Biotechnol.* 37:540–546.

839   Koren S, Walenz BP, Berlin K, Miller JR, Bergman NH, Phillippy AM. 2017. Canu: scalable and accurate
840   long-read assembly via adaptive k-mer weighting and repeat separation. *Genome Res.* 27:722–736.

841   Kumar S, Stecher G, Li M, Knyaz C, Tamura K. 2018. MEGA X: Molecular Evolutionary Genetics
842   Analysis across Computing Platforms. *Mol. Biol. Evol.* 35:1547–1549.

843   Kusaba M, Mochida T, Naridomi T, Fujita Y, Chuma I, Tosa Y. 2014. Loss of a 1.6 Mb chromosome in
844   Pyricularia oryzae harboring two alleles of AvrPik leads to acquisition of virulence to rice cultivars
845   containing resistance alleles at the Pik locus. *Curr. Genet.* 60:315–325.

846   Langner T, Harant A, Gomez-Luciano LB, Shrestha RK, Malmgren A, Latorre SM, Burbano HA, Win J,
847   Kamoun S. 2021. Genomic rearrangements generate hypervariable mini-chromosomes in host-
848   specific isolates of the blast fungus. *PLoS Genet.* 17:e1009386.

849   Langner T, Harant A, Kamoun S. 2019. Isolation of supernumerary mini-chromosomes from fungi for
850   enrichment sequencing v1. Available from: https://www.protocols.io/view/isolation-of-
851   supernumerary-mini-chromosomes-from-f-9t7h6rn

852   Latorre SM. 2024. smlatorreo/mChr_Moryzae: mChr_Moryzae. Available from:
853   https://zenodo.org/doi/10.5281/zenodo.10628812

854   Latorre SM, Langner T, Malmgren A, Win J, Kamoun S, Burbano HA. 2022. SNP calling parameters have
855   minimal impact on population structure and divergence time estimates for the rice blast fungus.
856   *bioRxiv* [Internet]:2022.03.06.482794. Available from:
857   https://www.biorxiv.org/content/10.1101/2022.03.06.482794

858   Latorre SM, Reyes-Avila CS, Malmgren A, Win J, Kamoun S, Burbano HA. 2020. Differential loss of
859   effector genes in three recently expanded pandemic clonal lineages of the rice blast fungus. *BMC*
860   *Biol.* 18:88.

861   Latorre SM, Were VM, Foster AJ, Langner T, Malmgren A, Harant A, Asuke S, Reyes-Avila S, Gupta DR,
862   Jensen C, et al. 2023. Genomic surveillance uncovers a pandemic clonal lineage of the wheat blast
863   fungus. *PLoS Biol.* 21:e3002052.

864   Letunic I, Bork P. 2021. Interactive Tree Of Life (iTOL) v5: an online tool for phylogenetic tree display
865   and annotation. *Nucleic Acids Res.* 49:W293–W296.

866   Li H. 2013. Aligning sequence reads, clone sequences and assembly contigs with BWA-MEM. *arXiv [q-*
867   *bio.GN]* [Internet]. Available from: http://arxiv.org/abs/1303.3997

868   Liu S, Lin G, Ramachandran SR, Cruppe G, Cook D, Pedley KF, Valent B. 2022. Rapid mini-chromosome
869   divergence among fungal isolates causing wheat blast outbreaks in Bangladesh and Zambia. *bioRxiv*
870   [Internet]:2022.06.18.496690. Available from:
871   https://www.biorxiv.org/content/10.1101/2022.06.18.496690.full

872   Ma L-J, van der Does HC, Borkovich KA, Coleman JJ, Daboussi M-J, Di Pietro A, Dufresne M, Freitag M,
873   Grabherr M, Henrissat B, et al. 2010. Comparative genomics reveals mobile pathogenicity
874   chromosomes in Fusarium. *Nature* 464:367–373.

875   Marçais G, Delcher AL, Phillippy AM, Coston R, Salzberg SL, Zimin A. 2018. MUMmer4: A fast and
876   versatile genome alignment system. *PLoS Comput. Biol.* 14:e1005944.

877   Masel AM, He C, Poplawski AM, Irwin JAG, Manners JM. 1996. Molecular evidence for chromosome
878   transfer between biotypes of Colletotrichum gloeosporioides. *Mol. Plant. Microbe. Interact.*
879   [Internet]. Available from: https://agris.fao.org/agris-search/search.do?recordID=US9632088

880   McCarthy CGP, Fitzpatrick DA. 2019. Pan-genome analyses of model fungal species. *Microb Genom*
881   [Internet] 5. Available from: http://dx.doi.org/10.1099/mgen.0.000243

882   McKenna A, Hanna M, Banks E, Sivachenko A, Cibulskis K, Kernytsky A, Garimella K, Altshuler D,
883   Gabriel S, Daly M, et al. 2010. The Genome Analysis Toolkit: a MapReduce framework for analyzing
884   next-generation DNA sequencing data. *Genome Res.* 20:1297–1303.

885   Mehrabi R, Bahkali AH, Abd-Elsalam KA, Moslem M, Ben M'barek S, Gohari AM, Jashni MK,
886   Stergiopoulos I, Kema GHJ, de Wit PJGM. 2011. Horizontal gene and chromosome transfer in plant
887   pathogenic fungi affecting host range. *FEMS Microbiol. Rev.* 35:542–554.

888   Mela AP, Rico-Ramírez AM, Glass NL. 2020. Syncytia in Fungi. *Cells* [Internet] 9. Available from:
889   http://dx.doi.org/10.3390/cells9102255

890   Miao VP, Covert SF, VanEtten HD. 1991. A fungal gene for antibiotic resistance on a dispensable ("B")
891   chromosome. *Science* 254:1773–1776.

892   Miller MA, Pfeiffer W, Schwartz T. 2010. Creating the CIPRES Science Gateway for inference of large
893   phylogenetic trees. In: 2010 Gateway Computing Environments Workshop (GCE). IEEE. p. 1–8.

894   Minh BQ, Schmidt HA, Chernomor O, Schrempf D, Woodhams MD, von Haeseler A, Lanfear R. 2020.
895   IQ-TREE 2: New Models and Efficient Methods for Phylogenetic Inference in the Genomic Era. *Mol.*
896   *Biol. Evol.* 37:1530–1534.

897   Mohanta TK, Bae H. 2015. The diversity of fungal genome. *Biol. Proced. Online* 17:8.

898   Möller M, Stukenbrock EH. 2017. Evolution and genome architecture in fungal plant pathogens. *Nat. Rev.*

899   *Microbiol.* 15:756–771.

900   Monsur MA, Kusaba M. 2018. Study on Parasexual Recombination between Pyricularia oryzae and
901   Pyricularia grisea. *Agric. Sci. China* 9:317–339.

902   Moolhuijzen PM, See PT, Shi G, Powell HR, Cockram J, Jørgensen LN, Benslimane H, Strelkov SE,
903   Turner J, Liu Z, et al. 2022. A global pangenome for the wheat fungal pathogen Pyrenophora tritici-
904   repentis and prediction of effector protein structural homology. *Microb Genom* [Internet] 8.
905   Available from: http://dx.doi.org/10.1099/mgen.0.000872

906   Nei M. 2007. The new mutation theory of phenotypic evolution. *Proc. Natl. Acad. Sci. U. S. A.* 104:12235–
907   12242.

908   Nieuwenhuis BPS, James TY. 2016. The frequency of sex in fungi. *Philos. Trans. R. Soc. Lond. B Biol. Sci.*
909   [Internet] 371. Available from: http://dx.doi.org/10.1098/rstb.2015.0540

910   Noguchi MT, Yasuda N, Fujita Y. 2006. Evidence of Genetic Exchange by Parasexual Recombination and
911   Genetic Analysis of Pathogenicity and Mating Type of Parasexual Recombinants in Rice Blast Fungus,
912   Magnaporthe oryzae. *Phytopathology* 96:746–750.

913   Oggenfuss U, Feurtey A, Reyes-Avila CS, Gluck-Thaler E, Puccetti G, Glad HM, Abraham LN, Stalder L,
914   Tralamazza SM, González-Sáyer SM, et al. 2023. Genome Evolution in Fungal Plant Pathogens: From
915   Populations to Kingdom-Wide Dynamics. In: Pöggeler S, James T, editors. Evolution of Fungi and
916   Fungal-Like Organisms. Cham: Springer International Publishing. p. 103–121.

917   Orbach MJ, Chumley FG, Valent B. 1996. Electrophoretic karyotypes of Magnaporthe grisea pathogens
918   of diverse grasses. *MPMI-Molecular Plant Microbe Interactions* 9:261–271.

919   Peng Z, Oliveira-Garcia E, Lin G, Hu Y, Dalby M, Migeon P, Tang H, Farman M, Cook D, White FF, et al.
920   2019. Effector gene reshuffling involves dispensable mini-chromosomes in the wheat blast fungus.
921   *PLoS Genet.* 15:e1008272.

922   Petersen C, Sørensen T, Nielsen MR, Sondergaard TE, Sørensen JL, Fitzpatrick DA, Frisvad JC, Nielsen
923   KL. 2023. Comparative genomic study of the Penicillium genus elucidates a diverse pangenome and
924   15 lateral gene transfer events. *IMA Fungus* 14:3.

925   Potgieter L, Feurtey A, Dutheil JY, Stukenbrock EH. 2020. On Variant Discovery in Genomes of Fungal
926   Plant Pathogens. *Front. Microbiol.* 11:626.

927   Quinlan AR, Hall IM. 2010. BEDTools: a flexible suite of utilities for comparing genomic features.
928   *Bioinformatics* 26:841–842.

929   Rahman MT, Sobur MA, Islam MS, Ievy S, Hossain MJ, El Zowalaty ME, Rahman AT, Ashour HM. 2020.
930   Zoonotic Diseases: Etiology, Impact, and Control. *Microorganisms* [Internet] 8. Available from:
931   http://dx.doi.org/10.3390/microorganisms8091405

932   Rahnama M, Novikova O, Starnes JH, Zhang S, Chen L, Farman ML. 2020. Transposon-mediated
933   telomere destabilization: a driver of genome evolution in the blast fungus. *Nucleic Acids Res.*
934   48:7197–7217.

935   Roca MG, Arlt J, Jeffree CE, Read ND. 2005. Cell biology of conidial anastomosis tubes in Neurospora
936   crassa. *Eukaryot. Cell* 4:911–919.

937　Roca MG, Davide LC, Mendes-Costa MC, Wheals A. 2003. Conidial anastomosis tubes in
938　　　　Colletotrichum. *Fungal Genet. Biol.* 40:138–145.

939　Roper M, Ellison C, Taylor JW, Glass NL. 2011. Nuclear and genome dynamics in multinucleate
940　　　　ascomycete fungi. *Curr. Biol.* 21:R786–R793.

941　Sagulenko P, Puller V, Neher RA. 2018. TreeTime: Maximum-likelihood phylodynamic analysis. *Virus Evol*
942　　　　4:vex042.

943　Sahu N, Indic B, Wong-Bajracharya J, Merényi Z, Ke H-M, Ahrendt S, Monk T-L, Kocsubé S, Drula E,
944　　　　Lipzen A, et al. 2023. Vertical and horizontal gene transfer shaped plant colonization and biomass
945　　　　degradation in the fungal genus Armillaria. *Nat Microbiol* [Internet]. Available from:
946　　　　http://dx.doi.org/10.1038/s41564-023-01448-1

947　Saleh D, Xu P, Shen Y, Li C, Adreit H, Milazzo J, Ravigné V, Bazin E, Nottéghem J-L, Fournier E, et al.
948　　　　2012. Sex at the origin: an Asian population of the rice blast fungus Magnaporthe oryzae
949　　　　reproduces sexually. *Mol. Ecol.* 21:1330–1344.

950　Schubert M, Lindgreen S, Orlando L. 2016. AdapterRemoval v2: rapid adapter trimming, identification,
951　　　　and read merging. *BMC Res. Notes* 9:88.

952　Scrucca L, Fraley C, Murphy TB, Raftery AE. 2023. Model-Based Clustering, Classification, and Density
953　　　　Estimation Using mclust in R. Chapman and Hall/CRC

954　Seidl MF, Thomma BPHJ. 2014. Sex or no sex: evolutionary adaptation occurs regardless. *Bioessays*
955　　　　36:335–345.

956　Simão FA, Waterhouse RM, Ioannidis P, Kriventseva EV, Zdobnov EM. 2015. BUSCO: assessing genome
957　　　　assembly and annotation completeness with single-copy orthologs. *Bioinformatics* 31:3210–3212.

958　Skoglund P, Mallick S, Bortolini MC, Chennagiri N, Hünemeier T, Petzl-Erler ML, Salzano FM, Patterson
959　　　　N, Reich D. 2015. Genetic evidence for two founding populations of the Americas. *Nature* 525:104–
960　　　　108.

961　Soanes D, Richards TA. 2014. Horizontal gene transfer in eukaryotic plant pathogens. *Annu. Rev.*
962　　　　*Phytopathol.* 52:583–614.

963　Stukenbrock EH. 2013. Evolution, selection and isolation: a genomic view of speciation in fungal plant
964　　　　pathogens. *New Phytol.* 199:895–907.

965　Stukenbrock EH. 2016. The Role of Hybridization in the Evolution and Emergence of New Fungal Plant
966　　　　Pathogens. *Phytopathology* 106:104–112.

967　Sun D. 2018. Pull in and Push Out: Mechanisms of Horizontal Gene Transfer in Bacteria. *Frontiers in*
968　　　　*Microbiology* [Internet] 9. Available from: http://dx.doi.org/10.3389/fmicb.2018.02154

969　Takeuchi N, Kaneko K, Koonin EV. 2014. Horizontal gene transfer can rescue prokaryotes from
970　　　　Muller's ratchet: benefit of DNA from dead cells and population subdivision. *G3* 4:325–339.

971　Talbot NJ, Salch YP, Ma M, Hamer JE. 1993. Karyotypic Variation within Clonal Lineages of the Rice
972　　　　Blast Fungus, Magnaporthe grisea. *Appl. Environ. Microbiol.* 59:585–593.

973　Thierry M, Charriat F, Milazzo J, Adreit H, Ravel S, Cros-Arteil S, Borron S, Sella V, Kroj T, Ioos R, et al.

974   2022. Maintenance of divergent lineages of the Rice Blast Fungus Pyricularia oryzae through niche
975   separation, loss of sex and post-mating genetic incompatibilities. *PLoS Pathog.* 18:e1010687.

976   Torres DE, Oggenfuss U, Croll D, Seidl MF. 2020. Genome evolution in fungal plant pathogens: looking
977   beyond the two-speed genome model. *Fungal Biol. Rev.* 34:136–143.

978   Tsujimoto Noguchi M. 2011. Parasexual recombination in Magnaporthe oryzae. *Jpn. Agric. Res. Q.* 45:39–
979   45.

980   Vangalis V, Knop M, Typas MA, Papaioannou IA. 2021. Establishment of conidial fusion in the asexual
981   fungus Verticillium dahliae as a useful system for the study of non-sexual genetic interactions. *Curr.*
982   *Genet.* 67:471–485.

983   Van Valen L. 1973. Patterns and the balance of nature. *Evolutionary Theory* 1:31–49.

984   Vaser R, Sović I, Nagarajan N, Šikić M. 2017. Fast and accurate de novo genome assembly from long
985   uncorrected reads. *Genome Res.* 27:737–746.

986   Vlaardingerbroek I, Beerens B, Rose L, Fokkens L, Cornelissen BJC, Rep M. 2016. Exchange of core
987   chromosomes and horizontal transfer of lineage-specific chromosomes in Fusarium oxysporum.
988   *Environ. Microbiol.* 18:3702–3713.

989   Walker BJ, Abeel T, Shea T, Priest M, Abouelliel A, Sakthikumar S, Cuomo CA, Zeng Q, Wortman J,
990   Young SK, et al. 2014. Pilon: an integrated tool for comprehensive microbial variant detection and
991   genome assembly improvement. *PLoS One* 9:e112963.

992   van Westerhoven A, Aguilera-Galvez C, Nakasato-Tagami G, Shi-Kunne X, Dijkstra J, de la Parte EM,
993   Carero EC, Meijer H, Feurtey A, Maryani N, et al. 2023. Segmental Duplications Drive the
994   Evolution of Accessory Regions in a Major Crop Pathogen. *bioRxiv* [Internet]:2023.06.07.544053.
995   Available from: https://www.biorxiv.org/content/10.1101/2023.06.07.544053v1?ct=

996   Wickham H. 2009. ggplot2: Elegant Graphics for Data Analysis. Springer Science & Business Media

997   Win J, Harant A, Malmgren A, Langner T, Shrestha R-K, Latorre SM, Were V, Talbot NJ, Burbano HA,
998   Picco AM, et al. 2020. Large scale genome assemblies of Magnaporthe oryzae rice isolates from
999   Italy. Available from: https://zenodo.org/record/4326823

1000   Wright S. 1951. The genetical structure of populations. *Ann. Eugen.* 15:323–354.

1001   Younas MU, Wang G, Du H, Zhang Y, Ahmad I, Rajput N, Li M, Feng Z, Hu K, Khan NU, et al. 2023.
1002   Approaches to Reduce Rice Blast Disease Using Knowledge from Host Resistance and Pathogen
1003   Pathogenicity. *Int. J. Mol. Sci.* [Internet] 24. Available from: http://dx.doi.org/10.3390/ijms24054985

1004   Zeigler RS, Scott RP, Leung H, Bordeos AA, Kumar J, Nelson RJ. 1997. Evidence of parasexual exchange
1005   of DNA in the rice blast fungus challenges its exclusive clonality. *Phytopathology* 87:284–294.

1006   Zielezinski A, Vinga S, Almeida J, Karlowski WM. 2017. Alignment-free sequence comparison: benefits,
1007   applications, and tools. *Genome Biol.* 18:186.